



Late Pleistocene paleohydrology near the boundary of the Sonoran and Chihuahuan Deserts, southeastern Arizona, USA

Jeffrey S. Pigati^{a,*}, Jordon E. Bright^b, Timothy M. Shanahan^{c,1}, Shannon A. Mahan^d

^aUniversity of Arizona Desert Laboratory, 1675 W. Anklam Road, Tucson, AZ 85745, United States

^bDepartments of Geology and Environmental Sciences, Northern Arizona University, Flagstaff, AZ 86011, United States

^cGeosciences Department, University of Arizona, Tucson, AZ 85721, United States

^dU.S. Geological Survey, Geologic Division, Denver Federal Center, Box 25046, MS-974, Denver, CO 80225, United States

ARTICLE INFO

Article history:

Received 3 June 2008

Received in revised form

11 September 2008

Accepted 25 September 2008

ABSTRACT

Ground-water discharge (GWD) deposits form in arid environments as water tables rise and approach or breach the ground surface during periods of enhanced effective precipitation. Where preserved, these deposits contain information on the timing and elevation of past ground-water fluctuations. Here we report on the investigation of a series of GWD deposits that are exposed in discontinuous outcrops along a ~150-km stretch of the San Pedro Valley in southeastern Arizona, near the boundary of the Sonoran and Chihuahuan Deserts. Chronologic, isotopic, geochemical, faunal assemblage (ostracodes and gastropods), and sedimentological evidence collectively suggest that the elevation of the regional water table in the valley rose in response to a change in climate ~50 ka ago and remained relatively high for the next ~35 ka before falling during the Bølling–Allerød warm period, rebounding briefly during the Younger Dryas cold event, and falling again at the onset of the Holocene. The timing of these hydrologic changes coincides closely with variations in $\delta^{18}\text{O}$ values of calcite from a nearby speleothem to the west and changes in lake levels at pluvial Lake Cochise to the east. Thus, in southeastern Arizona, the assumption that changes in climate are reflected in all aspects of the hydrologic cycle of a region simultaneously is validated. The timing of these changes also broadly coincides with variations in the GISP2 $\delta^{18}\text{O}$ record, which supports the hypothesis that atmospheric teleconnections existed between the North Atlantic and the deserts of the American Southwest during the late Pleistocene.

Published by Elsevier Ltd.

1. Introduction

As continental ice sheets waxed and waned during the late Pleistocene, global reorganizations of the atmosphere, biosphere, and hydrosphere resulted in dramatic physical changes in the deserts of the American Southwest. During full glacial times in the Sonoran and Chihuahuan Deserts, for example, elevations of plant communities were often displaced 1000 m or more downslope (King and Van Devender, 1977; Van Devender and Burgess, 1985; Van Devender, 1990a,b; Anderson and Van Devender, 1991; McAuliffe and Van Devender, 1998; Betancourt et al., 2001; Holmgren et al., 2003, 2006), large lake systems were present where only seasonally filled lakes or dry playas exist today (Long, 1966; Fleischhauer and Stone, 1982; Waters, 1989; Wilkins and

Currey, 1997; Krider, 1998; Allen and Anderson, 2000), and mega-fauna lived in areas that are now too hot and dry to support them (Haury et al., 1953, 1959; Harris, 1987; Ratkevich, 1993; Haynes and Huckell, 2007). The cooler, wetter conditions of the late Pleistocene also supported higher water tables in these deserts, which fed flowing springs, wet meadows, seeps, and wetlands in low-lying valley floors and adjacent tributaries (Ashbaugh and Metcalf, 1986; Haynes, 1987). As continental ice sheets retreated toward the end of the Pleistocene, the polar jet stream and associated storm tracks migrated to the north, and more arid conditions prevailed in the American Southwest (COHMAP, 1988; Thompson et al., 1993; Bartlein et al., 1998; Kutzbach et al., 1998). As a result, regional water tables fell, shallow valley fill aquifers dried up, tributary stream flow slowed or ceased, and erosive conditions eventually dominated (Waters and Haynes, 2001).

Traditionally, geologists have relied heavily on lake deposits to reconstruct the magnitude and timing of Late Quaternary climatic and hydrologic changes in the American Southwest. Additional paleohydrologic information is present in ground-water discharge deposits, also referred to as “paleospring” or “paleowetland” deposits (Forester et al., 2003). Ground-water discharge (GWD)

* Corresponding author. Present address: U.S. Geological Survey, Geologic Division, Denver Federal Center, Box 25046, MS-980, Denver, CO 80225, United States. Tel.: +1 303 236 7870; fax +1 303 236 5349.

E-mail address: jpigati@usgs.gov (J.S. Pigati).

¹ Present address: Woods Hole Oceanographic Institution, Fye 104, MS-4, Woods Hole, MA 02543, United States.

deposits form in arid environments as water tables rise and approach or breach the ground surface during periods of enhanced effective precipitation. These deposits can take many forms, but typically consist of a combination of carbonate and/or silicate precipitants, accumulations of organic matter, and fine-grained (often eolian) sediments. The specific physical and chemical nature of GWD deposits at a given location depends on a number of factors, including ground-water chemistry, water temperature, availability and mobility of surface waters, density of plants in and around the paleowetland system, and the degree of preservation. At these sites, the interplay between emergent water tables, ecological and biological systems, and eolian processes results in unique and complex depositional environments that contain information on the timing and magnitude of past changes in local or regional hydrologic budgets. The resulting deposits also clearly demarcate the position of past water tables on the landscape, providing direct evidence of wetter times.

GWD deposits have been identified in all four of the major deserts of North America (Chihuahuan, Great Basin, Mojave and Sonoran), but have been studied in detail at only a limited number of sites (Quade, 1986; Quade and Pratt, 1989; Haynes, 1991; Quade et al., 1995, 1998, 2003; Kaufman et al., 2002; Pedone and Rivera, 2003; Pigati et al., 2004; Mahan et al., 2007). GWD deposits offer several advantages over other sources of paleohydrologic information. First, GWD deposits can often be dated reliably by ^{14}C using the remains of vascular plants or small terrestrial gastropods, thus avoiding problems with carbon reservoir effects that can affect lake systems (Deevey et al., 1954; Geyh et al., 1998). Additional chronometric techniques, including uranium-series, luminescence, and amino-acid racemization dating, may also be utilized under favorable circumstances. Second, GWD deposits often crop out over extensive areas, which afford researchers the opportunity to examine and interpret complex features, such as cut-and-fill sequences and laterally variable depositional facies. Third, GWD deposits are relatively common features in valley floors and adjacent low-lying areas in deserts and, therefore, can be used to reconstruct paleohydrologic conditions on a variety of spatial and temporal scales. The prevalence of GWD deposits in arid environments allows reconstruction of hydrologic conditions along geographic and elevation transects, including areas not covered by either lakes or speleothems. Finally, GWD deposits often contain freshwater microfauna (ostracodes, diatoms) and gastropod shells, which can be used to reconstruct past environmental and hydrologic conditions.

The primary limitation of GWD deposits is that it is not possible to relate the magnitude of climate change, in terms of quantitative reconstruction of precipitation and evapotranspiration (P/ET), to changes in the local or regional hydrologic budget. Once a wetland system reaches a critical threshold, additional input via increased precipitation or decreased evapotranspiration is largely lost to overland flow. Modeling ground-water discharge via overland flow has been addressed in complex regional wetland systems (Restrepo et al., 1998) but not in small desert watersheds. Thus, much like lakes that overtop their spillways, the amount of water required to raise the water table up to the elevation of GWD deposits should be viewed as a *minimum* value. A second complicating factor is that desert springs and wetlands commonly act as discharge points of shallow aquifers that are semi-confined. Quantifying the relationship between water table levels and P/ET in a semi-confined aquifer is difficult because it depends largely on how well the permeability and conductivity of near surface sediments are understood.

In this study, we investigated a series of GWD deposits that are exposed in discontinuous outcrops along a ~150-km stretch of the San Pedro Valley in southeastern Arizona, near the boundary of the Sonoran and Chihuahuan Deserts (Fig. 1). The results of multiple chronometric techniques show that these GWD deposits represent

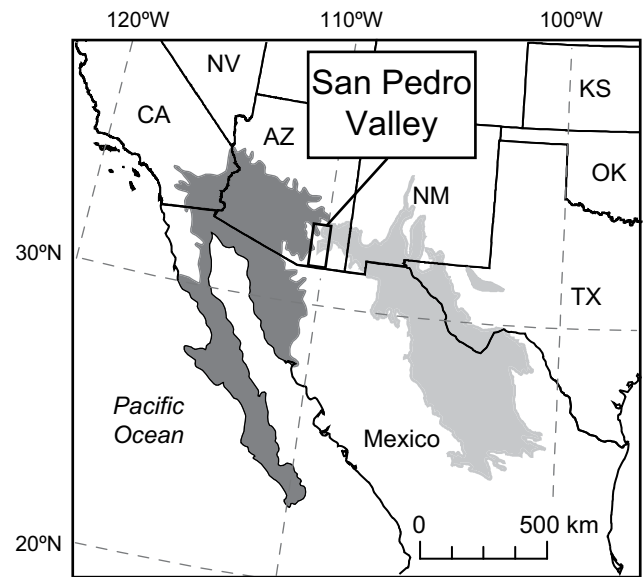


Fig. 1. Map of the American Southwest showing the location of the San Pedro Valley in relation to the Sonoran (darkly shaded) and Chihuahuan (lightly shaded) Deserts.

a period of enhanced effective precipitation that spanned much of oxygen isotope stages (OIS) 2 and 3. Chronologic, isotopic, geochemical, faunal assemblage (ostracodes and gastropods), and sedimentological evidence collectively suggest that the elevation of the regional water table in the San Pedro Valley rose in response to a change in climate ~50 ka ago and remained relatively high for the next ~35 ka before falling during the Bølling–Allerød warm period, rebounding briefly during the Younger Dryas cold event (YD), and falling again at the onset of the Holocene.

2. Regional setting

The San Pedro Valley is located in the southernmost portion of the Basin and Range Province of the western United States. Like most valleys in this province, the San Pedro Valley is aligned essentially north–south and extends from a few kilometers south of the International Border between the United States and Mexico to the Gila River basin, roughly 200 km to the north. Today, the valley is home to the San Pedro River, one of the last remaining undammed, unchannelized rivers in the American Southwest (Hanson, 2001). The San Pedro originates as rivulets and small streams that drain the Sierra de los Ajos and Sierra de la Mariquita in northern Sonora, increases in size and discharge after it crosses the International Border, and flows northward, dropping some 400 m in elevation across the ~150-km stretch of our study area.

Prior to the early 1900s, the San Pedro River flowed year-round, but today, the river channel's discharge alternates between gaining and losing, depending on the local depth to bedrock. Significant flow is generally limited to a short period (days to weeks) following summer thunderstorms, autumn tropical storms, and winter frontal storms (Pool and Coes, 1999). With a few modest exceptions, tributary channels and rivulets in the lower valley remain dry throughout the year.

The river system is fed by a regional aquifer that originates in the adjacent uplands on the west side of the valley, including the Huachuca, Whetstone, Rincon, and Santa Catalina Mountains (Fig. 2). These mountain ranges are comprised largely of Paleozoic sedimentary rocks (sandstone, limestone, and shale) that overlie pre-Cambrian granitoid basement rock (Reynolds, 1988). The Huachuca, Rincon, and Santa Catalina Mountains include peaks that exceed 3000 m in elevation; the Whetstone Mountains are slightly

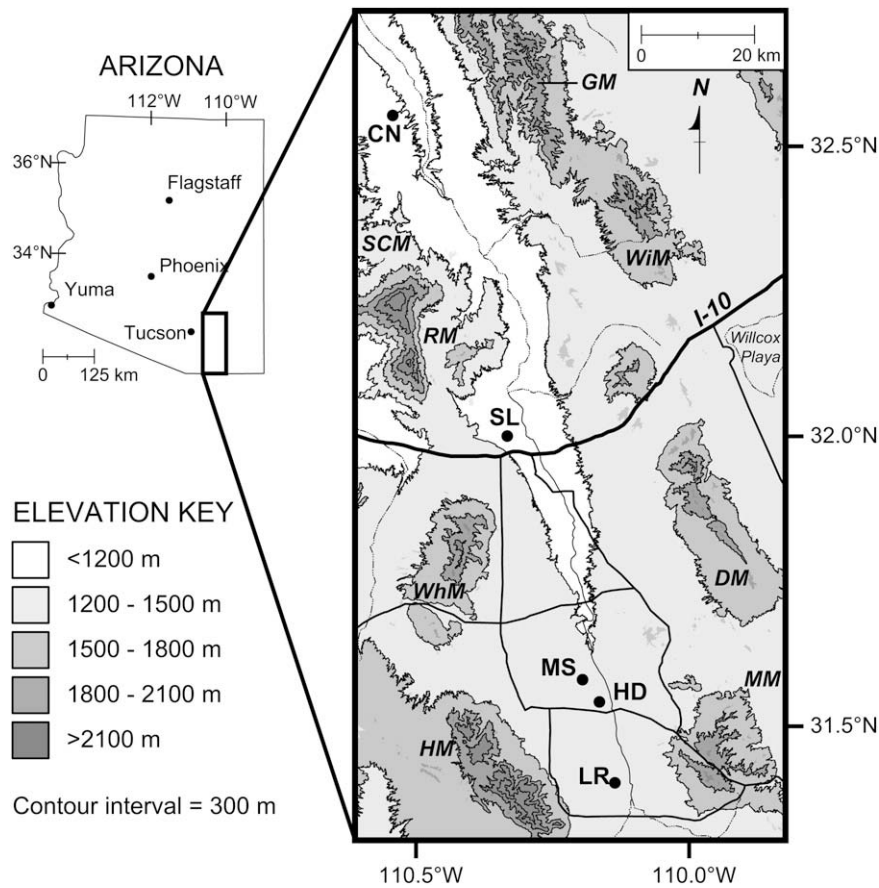


Fig. 2. Site location map for selected GWD deposits in the San Pedro Valley. The bottom of the figure is the location of the International Border between the United States and Mexico. State highways are shown for reference. Key for sites (filled circles; from south to north): LR = Lehner Ranch, HD = Horsethief Draw, MS = Murray Springs, SL = the Seff Locality, CN = Cerros Negros. Key for mountain ranges (italics; clockwise from lower left): HM = Huachuca Mountains, WhM = Whetstone Mountains, RM = Rincon Mountains, SCM = Santa Catalina Mountains, GM = Galiuro Mountains, WiM = Winchester Mountains, DM = Draoon Mountains, MM = Mule Mountains.

lower, peaking at ~2350 m. The ranges that flank the east side of the valley, including the Draoon, Winchester, and Mule Mountains, are lower, rarely exceeding 2000 m in elevation, and are comprised of Tertiary volcanics to the north and Mesozoic sedimentary rocks with local volcanics and Tertiary granitoids to the south (Reynolds, 1988).

Rapid headcutting and incision that occurred in the late 1800s precipitated a drop in water table levels in the San Pedro Valley and surrounding areas (Cooke and Reeves, 1976; Waters and Haynes, 2001). During this time, active wetlands in the American Southwest and northern Mexico largely disappeared (Minckley and Brunelle, 2007) and arroyos cut into alluvial fan sediments along the east flanks of the Huachuca, Rincon, and Santa Catalina Mountains, exposing an unusually complete sequence of Late Quaternary deposits at Curry Draw and other locations in the San Pedro Valley (Haynes, 1987). The exposed deposits include four members of the Murray Springs and Lehner Ranch Formations as defined by Haynes (1968) that are central to our study. They are, from oldest to youngest: the Coro Marl Member (Stratum E), the Graveyard Gulch Member (Stratum F1), the Clanton Ranch Member (Stratum F2; also known as the “black mat”), and the Earp Member (Stratum F2b; coeval with Stratum F2). We investigated these units at six sites, from south to north: Lehner Ranch, Horsethief Draw, Murray Springs (two sections), the Seff Locality, and Cerros Negros (Figs. 2 and 3, Table 1). Several of these sites were originally investigated as part of archeological or paleontological studies (Haury et al., 1959; Hemmings and Haynes, 1969; Mead et al., 1975; Haynes and Huckell, 2007; Hemmings, 2007). Here we present a brief physical description and summary of our

observations for each of these units. For a more detailed description of these and other Late Quaternary-age deposits in the San Pedro Valley, as well as a comprehensive treatment of the archeology, geology, paleontology, and paleoecology of the Clovis-age Paleindian site at Murray Springs, see Haynes and Huckell (2007).

The Coro Marl Member (Stratum E) of the Murray Springs Formation is a hard, white to light grey, calcareous silty clay unit that is between ~0.5 and 3 m thick at the Lehner Ranch, Horsethief Draw, Murray Springs, and Cerros Negros sites (Fig. 3). It is not exposed at the Seff Locality site. The appearance of the Coro marl is massive to blocky, and is interrupted by lenses of olive-green to brown clay partings that can be traced laterally for a few centimeters to up to ~10 m. The marl is composed of ~25–30% CaCO₃ and 70–75% fine sands, silts, and clays of varying composition (mainly silicates and carbonates) that appear to be largely eolian mixed with some fluvial sediments. Where paleospring locations have been identified, the calcareous marl pinches out within a few tens of meters of the spring orifices, suggesting that the mechanisms of carbonate precipitation are limited to a relatively small area downstream of the spring vents. The marl contains very little organic matter and no identifiable plant macrofossils, but fossil gastropods and ostracodes are common to abundant. At Murray Springs, terrestrial gastropod shells were used previously to date the Coro Marl Member to between ~25 and 13 ¹⁴C ka B.P. (Pigati et al., 2004). Similar ages were obtained by ¹⁴C dating of small amounts of organic material recovered from large blocks of the marl, as well as the marl carbonate itself, at Murray Springs and other sites in the valley (Haynes, 2007a).

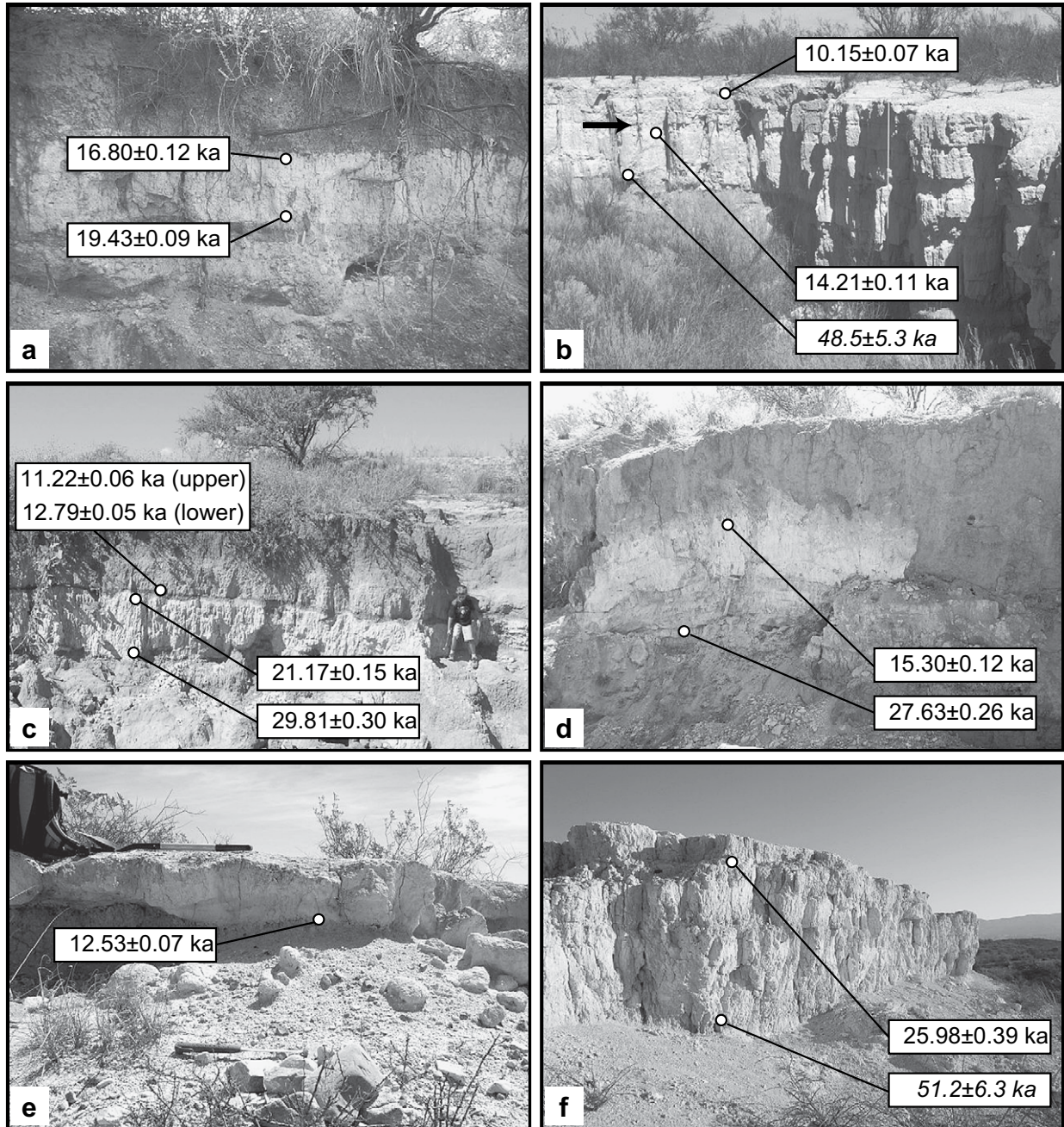


Fig. 3. Photographs of the Earp and Coro marls at (a) Lehner Ranch, (b) Horsethief Draw, (c) Murray Springs Section 1, (d) Murray Springs Section 2, (e) the Seff Locality, and (f) Cerros Negros. The arrow in Panel (b) points to the contact between the two marls at Horsethief Draw. Upper and lower limiting ages shown for each marl unit are based on calibrated ¹⁴C data (standard text) and luminescence ages (italics).

The Graveyard Gulch Member (Stratum F1) of the Murray Springs Formation overlies the Coro marl and consists of well-defined channel sands and gravels that cut through older units,

Table 1
Site location information.

Site name	Latitude (°N)	Longitude (°W)	Elevation (m ASL)	Marls present	Thickness (cm)
Lehner Ranch	31.422	110.115	1289	Coro	50
Horsethief Draw	31.556	110.160	1268	Earp Coro	90 225
Murray Springs #1	31.571	110.178	1270	Coro	110
Murray Springs #2	31.571	110.178	1270	Coro	80
Seff Locality	31.988	110.325	1130	Earp	25
Cerros Negros	32.536	110.558	951	Coro	385

including the Coro Marl Member. The basal contact of Stratum F1 is part of a widespread erosional surface (contacts Z₁ and Z₁₋₂ of Haynes (1984, 1998)) and is often represented as a disconformity between the underlying Coro marl and overlying sediments. Of the sites we investigated, the top of the Coro marl appears to be preserved only at Murray Springs #2 and Horsethief Draw (Fig. 3b, d). The marl is truncated at Lehner Ranch and Murray Springs #1 (Fig. 3a, c) and is exposed at the ground surface at Cerros Negros (Fig. 3f). Radiocarbon dates obtained by Haynes on charcoal (ash wood, *Fraxinus* sp.) recovered from the channel sands of Stratum F1 generally fall between ~12.9 and 10.7 ¹⁴C ka B.P. (Haynes, 2007a).

The Clanton Ranch Member (Stratum F2) of the Lehner Ranch Formation is comprised of an organic-rich silty clay and appears as a thin (2–10 cm) dark-brown or black stratum that conformably

overlies an earlier land surface, including the Clovis occupational surface, artifacts and kill sites, and remains of extinct megafauna. It has a sharp basal contact that is independent of the underlying lithology and pinches out ~1–2 m above the lowest areas (Haynes, 2007b). Numerous ^{14}C ages for the base-insoluble fraction (residue) of the Clanton clay at Murray Springs fall between ~10.8 and 9.7 ^{14}C ka B.P. (Haynes, 2007a). Base-soluble carbon compounds, mostly humic acids, typically yield ^{14}C ages that are slightly younger.

The Earp Member (Stratum F2b) of the Lehner Ranch Formation is a second marl unit that appears to have been deposited in local, low-lying areas and is coeval with the Clanton clay (the Earp marl and Clanton clay are different facies of the same time-stratigraphic unit). It is similar in appearance to the older Coro marl, but is usually softer and slightly darker (more grey than white), contains only dispersed fossil gastropod shells, and is stratigraphically and chronologically younger. Thin stringers of the Clanton clay are interbedded with the Earp marl in the ancient low areas at Murray Springs. At Horsethief Draw, however, the Earp marl is thick (~90 cm) and directly overlies the Coro marl where Strata F1 and F2 are missing (Fig. 3b). At the Seff Locality, the Earp marl is ~25 cm thick and overlies alluvial sediments (Fig. 3e). Previous radiocarbon dates for the Earp marl range from 10.3 ^{14}C ka B.P. (date on marl carbonate) to 9.0 ^{14}C ka B.P. (date on black mat stringer recovered from within the Earp marl) (Haynes, 2007c).

3. Materials and methods

3.1. Chronology

3.1.1. Radiocarbon dating

Terrestrial gastropod shells were collected for radiocarbon dating in 2000 (Murray Springs #1), 2001 (Murray Springs #2, Cerros Negros), 2002 (Lehner Ranch, Horsethief Draw), 2005 (the Seff Locality), and 2007 (Horsethief Draw again). During each site visit, the Coro and Earp marls were too indurated to allow handpicking of individual shells in the field. Therefore, we collected samples of the calcareous sediment in ~10-cm blocks at Murray Springs and 5- to 20-cm blocks at Lehner Ranch, Horsethief Draw, the Seff Locality, and Cerros Negros and processed them in the laboratory.

We recovered shells of a number of terrestrial, semi-aquatic, and aquatic gastropods from the marl at each site using the techniques described in Appendix A.1, but limited our focus to the terrestrial gastropods *Pupilla muscorum* and *Euconulus fulvus*, and the semi-aquatic gastropod family Succineidae for dating purposes. These taxa appear to yield reliable ^{14}C ages in arid environments even when living on limestone strata or adjacent to flowing springs (Pigati et al., 2004). Other terrestrial gastropod taxa are known to incorporate carbon derived from limestone when building their shells and, therefore, would yield ^{14}C ages that are anomalously old (e.g., Goodfriend and Stipp, 1983). Similarly, aquatic gastropods are subject to carbon reservoir effects, which can be significant in spring-discharge settings (Riggs, 1984), and were not considered for ^{14}C dating.

Radiocarbon ages corrected for fractionation are reported in ^{14}C years using the Libby half-life (5568 ± 30 years) (Libby, 1955) and, after calibration, in calendar years using the Cambridge half-life (5730 ± 40 years) (Mann et al., 1961; Watt et al., 1961; Karlen and Olsson, 1962) (Table 2). For calibration, we used both the Fairbanks0107 marine calibration dataset (<http://radiocarbon.ldeo.columbia.edu/research/radcarbcal.htm>, accessed 20 February 2008, Fairbanks et al., 2005) and the IntCal04.14C dataset (CALIB 5.1.0.Beta, Stuiver and Reimer, 1993; Reimer et al., 2004). Hereafter, we use ages determined using the Fairbanks calibration dataset in our discussions because nearly half of our ^{14}C ages are beyond the limit of the IntCal04.14C dataset (26 ka B.P.). We note that we did

not find any significant differences in the calibrated ages between the two programs for samples younger than this limit (Table 2). Uncertainties are reported at the 68% (1σ) confidence level. Stable carbon isotope values are reported in the usual delta (δ) notation as the per mil (‰) deviation from the VPDB standard. Analytical uncertainties for $\delta^{13}\text{C}$ measurements are less than 0.1‰ based on repeated measurements of standards.

3.1.2. Luminescence dating

Samples for luminescence dating were collected from the Coro marl in 2007 at Murray Springs (PVC tubes), Horsethief Draw (blocks) and Cerros Negros (blocks), and again in 2008 at Horsethief Draw (blocks). Analyses were carried out in subdued orange-light conditions at the U.S. Geological Survey's Luminescence Dating Laboratory in Denver, CO by one of us (SAM).

A minimum of the outermost two centimeters of sediment was removed from each sample to avoid dating sediments that may have been partially bleached during collection (Appendix A.2). Samples were treated with 10% HCl and 30% H_2O_2 to remove carbonate and organic matter, respectively, and then sieved and subjected to Stoke's settling to extract the 4–11 μm -size fraction because the marl samples were essentially devoid of sand-size grains. All samples reacted violently to the acid treatment, which took 24–48 h to complete. It was not possible to separate the quartz and feldspar grains because of the fine grain size and, therefore, we used a mixture of minerals for dating.

Infrared stimulated luminescence (IRSL) was performed using the total-bleach multiple-aliquot additive-dose (MAAD) method (Singhvi et al., 1982; Lang, 1994; Richardson et al., 1997; Forman and Pierson, 2002). Dose rates were determined based on concentrations of K, Rb, U, and Th, which were measured using instrumental neutron activation (INAA) at the U.S. Geological Survey's INAA laboratory in Denver, CO. Samples collected at Murray Springs were also measured for K, U, and Th by gamma spectrometry at the U.S.G.S. Luminescence Dating Laboratory. The cosmic-ray dose rate was estimated for each sample as a function of depth, altitude and geomagnetic latitude and added to the total dose rate (Prescott and Hutton, 1994). Alpha and beta contributions to the dose rate were corrected for grain-size attenuation as needed (Aitken, 1985). Concentrations of K, Rb, U, and Th, which contribute most of the ionizing radiation in the sediment, and the cosmic-ray dose rate were similar for all samples except those collected near the base of the Coro marl at Cerros Negros, where the radioisotope concentrations were higher (Table 3).

Anomalous fading tests were performed to account for the instability in the measured luminescence signal. Values obtained from these tests consist of a ratio of the initial luminescence emission and the emission measured after storage of a sample for 30–60 days after the initial measurement; a ratio of 1 indicates a stable luminescence signal (Huntley and Lamothe, 2001). Most samples exhibited a fairly stable signal, but samples CN-IRSL-1a, -1b, and -2 required a substantial correction to account for fading (Table 3). These samples were collected at Cerros Negros near the basal contact between the Coro marl and the underlying alluvial sediments, which included abundant Tertiary volcanic clasts. It is likely that fine-grained volcanic clasts, which are often associated with unstable luminescence signals and fading problems, were reworked from the unit below and deposited within the marl at this location. Feldspars present in the other samples appear to be from plutonic source(s) and, therefore, significant corrections for fading anomalies were not required.

3.2. Stable isotopes ($\delta^{13}\text{C}$, $\delta^{18}\text{O}$)

3.2.1. Marl carbonate

We collected ~3-g samples of marl carbonate in 2001 at Murray Springs and 2007 at Lehner Ranch, Horsethief Draw, the Seff

Table 2
Summary of ^{14}C results.

Sample	AMS #	Source ^a	Gastropod taxa ^b	Marl	Depth ^c (cm)	$\delta^{13}\text{C}$ (vpdb)	^{14}C age (ka)	Calibrated ages (ka B.P.)		
								Fairbanks ^d	CALIB ^e	p^f
<i>Lehner Ranch</i>										
SPV02-LR1-3	AA61001	1	Succineidae ($n = 5$)	Coro	0–10	–5.4	14.30 ± 0.05	16.80 ± 0.12	17.11 ± 0.21	1.00
SPV02-LR1-1a	AA60999	1	Succineidae ($n = 5$)	Coro	40–50	–4.4	16.31 ± 0.07	19.43 ± 0.09	19.46 ± 0.06	1.00
<i>Horsethief Draw</i>										
SPV02-HD1-7	AA61002	1	Succineidae ($n = 1$)	Earp	25–35	–5.9	8.95 ± 0.04	10.15 ± 0.07	9.97 ± 0.02	0.30
									10.02 ± 0.01	0.06
									10.05 ± 0.01	0.12
									10.17 ± 0.03	0.52
SPV07-HD1-7	AA75491	1	Multiple taxa ^g	Earp	25–35	–6.0	9.01 ± 0.04	10.20 ± 0.03	10.21 ± 0.02	1.00
SPV07-HD1-4c	AA75490	1	<i>Euconulus fulvus</i> ($n = 6$)	Coro	10–20	–6.4	12.37 ± 0.05	14.21 ± 0.11	14.31 ± 0.17	1.00
SPV07-HD1-4b	AA75489	1	Succineidae ($n = 8$)	Coro	10–20	–5.4	12.41 ± 0.05	14.29 ± 0.13	14.37 ± 0.14	0.84
									14.55 ± 0.03	0.16
SPV07-HD1-4a	AA75488	1	Succineidae ($n = 3$)	Coro	10–20	–6.0	12.66 ± 0.05	14.75 ± 0.10	14.95 ± 0.13	1.00
SPV02-HD1-1a	AA53122	1	Succineidae ($n = 7$)	Coro	150–160	–6.4	36.07 ± 0.43	41.32 ± 0.42	–	–
SPV02-HD1-1a	AA53123	1	<i>Pupilla muscorum</i> ($n = 7$)	Coro	150–160	–5.1	36.59 ± 0.70	41.78 ± 0.64	–	–
<i>Murray Springs – Section 1</i>										
SPV00-MS1-1a	AA39316	2	Succineidae ($n = 2$)	Coro	0–10	–6.5	17.86 ± 0.08	21.17 ± 0.15	21.10 ± 0.20	1.00
SPV00-MS1-1b	AA39317	2	Succineidae ($n = 8$)	Coro	0–10	–6.5	18.16 ± 0.08	21.61 ± 0.16	21.63 ± 0.23	1.00
SPV00-MS1-2	AA39326	2	Succineidae ($n = 5$)	Coro	10–20	–5.8	19.38 ± 0.11	23.06 ± 0.20	23.03 ± 0.26	1.00
SPV00-MS1-3	AA39327	2	Succineidae ($n = 9$)	Coro	20–30	–5.7	21.03 ± 0.10	25.17 ± 0.15	25.09 ± 0.07	0.25
									25.43 ± 0.12	0.75
SPV00-MS1-4	AA39319	2	Succineidae ($n = 7$)	Coro	30–40	–5.7	21.60 ± 0.12	25.98 ± 0.18	–	–
SPV00-MS1-5	AA39328	2	Succineidae ($n = 8$)	Coro	40–50	–5.6	23.57 ± 0.12	28.25 ± 0.19	–	–
SPV00-MS1-6	AA39329	2	Succineidae ($n = 10$)	Coro	50–60	–5.5	23.69 ± 0.13	28.39 ± 0.20	–	–
SPV00-MS1-7	AA39330	2	Succineidae ($n = 7$)	Coro	60–70	–4.8	24.42 ± 0.14	29.21 ± 0.20	–	–
SPV00-MS1-8	AA39331	2	Succineidae ($n = 4$)	Coro	70–80	–5.5	24.98 ± 0.14	30.00 ± 0.26	–	–
SPV00-MS1-9a	AA39318	2	Succineidae ($n = 2$)	Coro	80–90	–6.6	24.47 ± 0.12	29.26 ± 0.18	–	–
SPV00-MS1-9f	AA47648	2	<i>Euconulus fulvus</i> ($n = 5$)	Coro	80–90	–6.8	24.74 ± 0.20	29.63 ± 0.32	–	–
SPV00-MS1-9e	AA47647	2	<i>Pupilla muscorum</i> ($n = 5$)	Coro	80–90	–6.8	25.70 ± 0.21	30.91 ± 0.26	–	–
SPV00-MS1-10	AA39333	2	Succineidae ($n = 8$)	Coro	90–100	–6.2	24.62 ± 0.14	29.45 ± 0.22	–	–
SPV00-MS1-11a	AA39320	2	Succineidae ($n = 2$)	Coro	100–110	–6.3	24.31 ± 0.18	29.08 ± 0.24	–	–
SPV00-MS1-11b	AA39321	2	Succineidae ($n = 8$)	Coro	100–110	–6.3	24.86 ± 0.17	29.81 ± 0.30	–	–
<i>Murray Springs – Section 2</i>										
SPV01-MS2-6	AA47649	2	<i>Euconulus fulvus</i> ($n = 9$)	Coro	0–12	–6.6	13.14 ± 0.06	15.30 ± 0.12	15.53 ± 0.17	1.00
SPV01-MS2-6	AA43399	2	Succineidae ($n = 4$)	Coro	0–12	–6.0	13.68 ± 0.08	15.92 ± 0.14	16.28 ± 0.21	1.00
SPV01-MS2-9	AA43400	2	Succineidae ($n = 4$)	Coro	37–49	–5.9	19.78 ± 0.12	23.64 ± 0.17	23.69 ± 0.19	1.00
SPV01-MS2-12	AA43401	2	Succineidae ($n = 9$)	Coro	73–85	–6.0	23.02 ± 0.20	27.63 ± 0.26	–	–
<i>Seff Locality</i>										
SPV05-SL-1	AA65899	1	Succineidae ($n = 2$)	Earp	30–35	–7.3	10.57 ± 0.06	12.53 ± 0.07	12.43 ± 0.03	0.29
									12.67 ± 0.08	0.71
<i>Cerros Negros</i>										
SPV01-CN1-2	AA45849	1	Succineidae ($n = 2$)	Coro	15–35	–5.5	21.62 ± 0.28	25.98 ± 0.39	–	–
SPV01-CN1-8	AA49850	1	Succineidae ($n = 3$)	Coro	375–385	–6.9	38.5 ± 1.9	43.4 ± 1.7	–	–

Uncertainties for the raw and calibrated ^{14}C ages are given at the 1σ (68%) confidence level.

^a 1 = this study, 2 = Pigati et al. (2004).

^b Number of shells used for ^{14}C dating given in parentheses.

^c Depth from the top of each marl (Coro, Earp).

^d Fairbanks0107 dataset; limit 50.0 calendar ka B.P.; <http://radiocarbon.ldeo.columbia.edu/research/radcal.htm> (accessed 15.02.08).

^e CALIB v. 5.1.0.Beta, IntCal04.14C dataset; limit 26.0 calendar ka B.P. Calibrated ages are reported as the midpoint of the calibrated range. Uncertainties are reported as the difference between the midpoint and either the upper or lower limit of the calibrated age range, whichever is greater. Multiple ages are reported when the probability of a calibrated age range exceeded 0.05.

^f p = probability of the calibrated age falling within the reported range as calculated by CALIB.

^g Succineidae fragments ($n = 2$), *Gyraulus parvus* ($n = 6$), *Gastrocopta pentodon* ($n = 7$).

Locality, and Cerros Negros in 2- to 5-cm increments from each of the exposed marl sections (Coro and Earp). Aliquots were selected for analysis after homogenization with a mortar and pestle to minimize the effect of intrasample variability (Appendix A.3). Marl carbonate was converted to CO_2 using 100% H_3PO_4 under vacuum at 70 °C. Stable isotopes ($\delta^{18}\text{O}$, $\delta^{13}\text{C}$) were measured on a Finnigan MAT 252 mass spectrometer equipped with a Kiel III automated sampling device². As above, measured $\delta^{13}\text{C}$ and $\delta^{18}\text{O}$ values of the marl carbonate are reported in the usual delta (δ) notation as the per mil (‰) deviation from the VPDB standard. Analytical uncertainties for the $\delta^{18}\text{O}$ and $\delta^{13}\text{C}$ values reported here are less than 0.1‰ based on repeated measurements of carbonate standards. In

all, we measured the $\delta^{13}\text{C}$ and $\delta^{18}\text{O}$ values of 281 samples of marl carbonate from the Earp and Coro marls at Horsethief Draw, Murray Springs (two sections), the Seff Locality, and Cerros Negros.

3.2.2. Ostracodes

For analysis of the stable isotopic composition ($\delta^{13}\text{C}$, $\delta^{18}\text{O}$) of ostracode calcite, we collected sediment samples in 2007 at Murray Springs in 5-cm blocks at four chronologic intervals: early glacial (29.5 ka B.P.; sample MS1-90–95), full glacial (24.8 ka B.P.; sample MS1-25–30), last glacial maximum (LGM; 20.9 ka B.P.; sample MS2-30–35), and late glacial (15.0 ka B.P.; sample MS2-0–5). Ostracodes were separated from the marl sediment by soaking and gently agitating in a weak sodium bicarbonate–sodium hexametaphosphate solution for up to a week, and then washed with hot water over 150 μm sieves. Individual ostracode valves were hand-picked, sonicated gently, rinsed with deionized water, and dried

² Any use of trade, product, or firm names is for descriptive purposes and does not imply endorsement by the U.S. Government.

Table 3
Summary of IRSL results.

Sample ID	Depth cm	% Water content ^a	K (%) ^b	Rb (ppm) ^b	Th (ppm) ^b	U (ppm) ^b	Cosmic dose ^c (Gy/ka)	Total dose (Gy/ka)	Equivalent Dose (Gy)	Raw age (ka B.P.) ^d	Corrected age (ka B.P.) ^e
<i>Horsethief Draw</i>											
HD-IRSL-2	110–120	6 (30)	0.58 ± 0.08	13.5 ± 0.5	3.05 ± 0.03	1.76 ± 0.04	0.23 ± 0.01	1.95 ± 0.11	31.1 ± 3.2	15.9 ± 1.9	18.0 ± 2.2
HD-IRSL-4	265–275	2 (33)	0.23 ± 0.05	32.2 ± 0.6	2.48 ± 0.03	1.02 ± 0.03	0.19 ± 0.01	1.12 ± 0.07	47.8 ± 2.4	42.7 ± 2.4	47.8 ± 2.9
HD-IRSL-1	265–275	2 (33)	0.23 ± 0.05	32.2 ± 0.6	2.48 ± 0.03	1.02 ± 0.03	0.19 ± 0.01	1.12 ± 0.07	49.1 ± 2.1	43.8 ± 4.8	48.5 ± 5.3
<i>Murray Springs</i>											
MS1-IRSL-2	0–5	7 (30)	0.57 ± 0.08	30.7 ± 0.7	3.63 ± 0.03	1.52 ± 0.03	0.23 ± 0.01	1.63 ± 0.07	24.6 ± 0.7	15.1 ± 1.1	16.8 ± 1.2
MS1-IRSL-1	105–110	7 (28)	0.53 ± 0.08	31.3 ± 0.8	4.24 ± 0.04	1.90 ± 0.04	0.20 ± 0.01	2.08 ± 0.10	51.1 ± 3.1	24.6 ± 2.7	27.6 ± 3.0
<i>Cerro Negro</i>											
CN-IRSL-4	70–80	3 (31)	0.54 ± 0.05	25.8 ± 0.6	2.86 ± 0.03	1.14 ± 0.03	0.23 ± 0.01	1.60 ± 0.06	36.3 ± 1.3	22.7 ± 0.9	24.8 ± 1.0
CN-IRSL-3	145–155	5 (33)	0.53 ± 0.08	25.1 ± 0.7	2.15 ± 0.02	1.22 ± 0.03	0.21 ± 0.01	1.52 ± 0.07	36.2 ± 2.9	23.8 ± 1.0	26.9 ± 1.2
CN-IRSL-2	255–265	6 (32)	1.44 ± 0.14	76.7 ± 1.3	7.84 ± 0.06	2.02 ± 0.03	0.18 ± 0.01	3.42 ± 0.13	52.7 ± 0.5	15.4 ± 1.2	35.1 ± 2.8
CN-IRSL-1a	365–375	4 (29)	1.57 ± 0.15	94.4 ± 1.3	8.03 ± 0.06	2.14 ± 0.04	0.15 ± 0.01	3.59 ± 0.14	76.4 ± 0.8	21.3 ± 1.7	50.4 ± 4.1
CN-IRSL-1b	365–375	4 (29)	1.57 ± 0.15	94.4 ± 1.3	8.03 ± 0.06	2.14 ± 0.04	0.15 ± 0.01	3.59 ± 0.14	77.6 ± 3.6	21.6 ± 2.6	51.2 ± 6.3

Uncertainties for all data, including the raw and corrected luminescence ages, are given at the 1 σ (68%) confidence level.

^a Sample moisture (percent sample saturation). Ages were calculated using 50% of the saturation moisture.

^b Measured by neutron activation analyses. Murray Springs data were checked via gamma spectrometry (low resolution NaI detector).

^c Cosmic doses and attenuation with depth were calculated using the methods of Prescott and Hutton (1994). See text for details.

^d Range of grain size was fixed at 4–11 microns due to the extremely fine-grained nature of sediment. Exponential fit used for equivalent dose data.

^e All samples except CN-IRSL-1a, b, and 2 were calculated using a fade correction of $g = 1.7\text{--}2.2\%$ per decade. The corrected ages for these three samples were calculated using a fade correction of $g = 10.2\%$ per decade.

under laminar flow before identification by one of us (JEB). Ostracodes that were present in significant numbers (>10 specimens in a sample) included three species of the genus *Candona* (one large and one small unknown species, and *Candona stagnalis*), two species of the genus *Cypridopsis* (*Cypridopsis okeechobei*, *Cypridopsis vidua*), *Scottia* sp., and *Strandesia meadensis*. Some of these taxa were large enough that only a single valve was required for analysis; others required multiple valves for each measurement. As above, all stable isotope measurements of ostracode calcite were performed using the Finnigan MAT 252 mass spectrometer equipped with a Kiel III automated sampling device. Analytical uncertainties for most of the $\delta^{18}\text{O}$ and $\delta^{13}\text{C}$ values reported here are less than 0.1‰. However, some of the ostracode samples (<6% of the total) were exceptionally small and required additional processing; uncertainties for these samples were 0.15‰ for $\delta^{13}\text{C}$ and 0.2‰ for $\delta^{18}\text{O}$. We did not observe any systematic biases in the ostracode isotopic values related to sample size. In all, we measured the isotopic values of 376 aliquots of ostracode calcite.

4. Results

4.1. Chronology and depositional rates

The basal age of the Coro Marl was determined using ^{14}C and luminescence dating techniques (Tables 2 and 3). Radiocarbon results show that the oldest ages from Horsethief Draw (41.78 ± 0.64 ka) and Cerros Negros (43.4 ± 1.7 ka) are at or near the limit of standard ^{14}C dating. Luminescence ages from the base of the marl at these sites indicate that marl deposition probably began a few thousand years earlier, by 48.5 ± 5.3 ka at Horsethief Draw and 51.2 ± 6.3 ka at Cerros Negros. The discrepancy between the ^{14}C and luminescence ages likely reflects the influence of a small amount (<1%) of modern carbon contamination, which causes ^{14}C ages to be younger than the actual ages. This can occur by the addition of secondary carbonate or by dissolution–recrystallization processes; both result in the formation of calcite within the aragonite shell matrix, but at levels that are well below the detection capabilities of X-ray diffraction (XRD). Apparent “finite” ^{14}C ages obtained from small terrestrial gastropod shells that are in excess of 50 ka have been documented previously in wetland systems in Southern Nevada (Quade et al., 2003) and in a lake shoreline setting in the Bolivian Altiplano (Placzek et al., 2006). This suggests that the practical limit of ^{14}C dating of shell carbonate in

some depositional environments is significantly lower than analytical limits. To date, the practical limits of ^{14}C dating of shell carbonate have not been rigorously addressed and, therefore, we prefer the basal dates obtained by luminescence dating and conclude that deposition of the Coro marl began ~ 50 ka ago.

The upper age of the Coro marl was determined by ^{14}C dating of gastropod shells at Murray Springs #2 (15.30 ± 0.12 ka) and Horsethief Draw (14.21 ± 0.11 ka). We take the midpoint of these two ages, 14.7 ka B.P., as the upper limiting age of the Coro Marl for four reasons: (1) to minimize the possible effects of a small degree of open-system behavior of the shell carbonate (this would make the ages younger), (2) similarly, incorporation of a small amount of old carbon during shell formation while the gastropods were still alive would make the ages slightly older, (3) there may be differences in response times between a climate event (i.e., a change in P or E/T) and ground-water discharge at each site, and (4) other potential factors related to site-specific characteristics that might affect the chronologic data obtained from each site to a small degree.

The Coro marl was deposited more or less continuously at our study sites as evidenced by the lack of erosional unconformities or depositional hiatuses within the unit. Deposition rates of the marl calculated by linear interpolation between fixed points (dated intervals) were generally between ~ 4 and 8 cm/ka, except for a brief period between ~ 25 and 30 ka B.P. when depositional rates temporarily increased to ~ 15 and 35 cm/ka at Murray Springs and Cerros Negros, respectively (Fig. 4).

The basal age of the Clanton clay and Earp marl (different facies of the same time-stratigraphic unit) is constrained by a ^{14}C age from gastropod shell carbonate from the Earp marl at the Seff Locality (12.53 ± 0.07 ka) and ^{14}C ages of the base-insoluble residue of organic samples of the Clanton clay at Murray Springs (12.79 ± 0.05 kyr, Haynes, 2007a). As above, we take the midpoint of these ages, 12.6 ka B.P., as the basal age of this unit.

The upper limiting age of the Clanton clay/Earp marl was determined by ^{14}C dating of gastropod shell carbonate at Horsethief Draw (10.15 ± 0.07 ka) and ^{14}C dating of the base-insoluble residue of organic samples at Murray Springs (11.22 ± 0.06 kyr, Haynes, 2007a). Again we take the midpoint, 10.6 ka B.P., as the upper age of this unit.

The Earp marl appears to have been deposited more rapidly than the older Coro marl, ~ 26 cm/ka at Horsethief Draw and ~ 13 cm/ka at the Seff Locality. However, we urge caution in taking these rates at face value because we were not able to obtain bracketing ages at

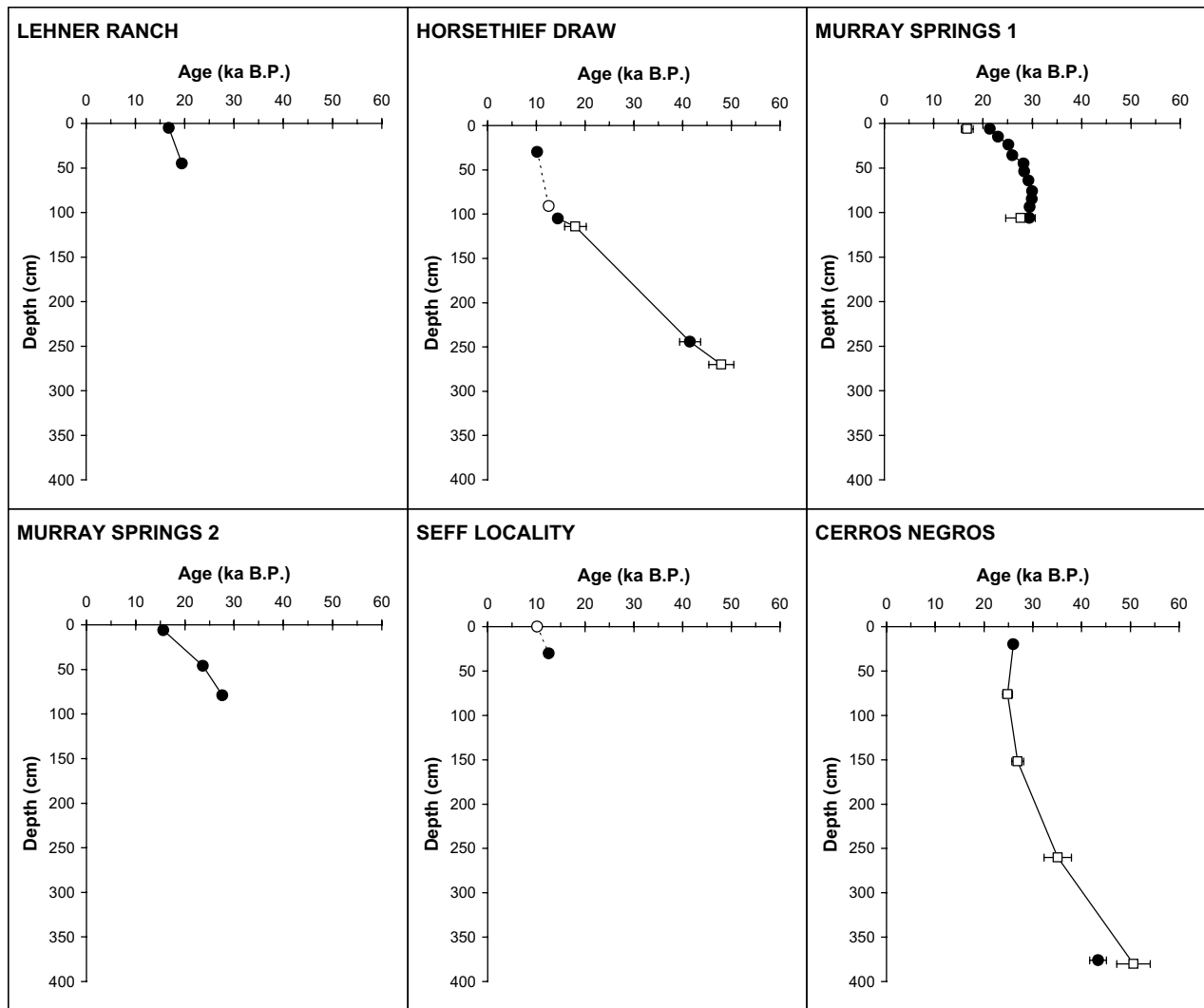


Fig. 4. Age models for GWD deposits at six sites in the San Pedro Valley. Calibrated ages based on ^{14}C measurements are shown as solid circles. Open circles denote inferred ages based on ^{14}C measurements made at other sites; the base and top of the Earp marl were constrained by ^{14}C ages at the Seff Locality and Horsethief Draw, respectively. Luminescence ages are represented by open squares. Linear interpolations between fixed points are shown for the Coro marl (solid lines) and Earp marl (dashed lines).

either site. The basal age of the Earp marl was taken at the Seff Locality, whereas the upper limiting age was taken at Horsethief Draw (shell ^{14}C age) and Murray Springs (organic ^{14}C ages). We assume coeval precipitation of the marl at these locations, which allows us to calculate a deposition rate, but this has not been verified with chronologic data.

4.2. Stable isotopes

4.2.1. Marl carbonate

$\delta^{18}\text{O}$ values obtained from the Coro marl carbonate range from -9.8 to -6.7‰ (Fig. 5). At Horsethief Draw and Cerros Negros, $\delta^{18}\text{O}$ values of the Coro marl carbonate are $\sim -9\text{‰}$ near the base of both sections. At Horsethief Draw, $\delta^{18}\text{O}$ values then quickly increase to $\sim -8\text{‰}$ and generally remain $\sim 0.5\text{‰}$ higher than those at Cerros Negros as oxygen isotope values at both sites increase slightly until ~ 28 ka B.P. Marl deposition began at Murray Springs at about this time, and $\delta^{18}\text{O}$ values there increase steadily between ~ 28 and 15 ka B.P. except for a small, brief negative excursion at Murray Springs #1 centered at ~ 25 ka B.P. In contrast, $\delta^{18}\text{O}$ values at Horsethief Draw remain relatively constant between ~ 27 and 14 ka B.P. $\delta^{18}\text{O}$ values from the youngest sections of the Coro marl are nearly identical (-8‰) at both Horsethief Draw and Murray

Springs #2. In all, the $\delta^{18}\text{O}$ of the Coro marl carbonate shows a general trend in which values increase slightly ($\sim 1\text{--}2\text{‰}$) between ~ 50 and 15 ka B.P.

Stable carbon isotopic values ($\delta^{13}\text{C}$) of the Coro marl carbonate are essentially constant between ~ 50 and 25 ka B.P., and then increase by $\sim 1\text{‰}$ between ~ 25 and 15 ka B.P. at all sites. This progression is interrupted by a positive excursion at Cerros Negros centered at ~ 37 ka B.P. This excursion, in which $\delta^{13}\text{C}$ values abruptly spike by $\sim 2\text{‰}$, is not seen in any of the other Coro marl $\delta^{13}\text{C}$ records. The positive trend in both $\delta^{18}\text{O}$ and $\delta^{13}\text{C}$ values at the top of the Cerros Negros record is likely due to diagenetic effects as the top of the Coro marl at this location is exposed at the ground surface.

Finally, unlike the isotopic values of the Coro Marl, $\delta^{18}\text{O}$ and $\delta^{13}\text{C}$ values of the Earp marl carbonate covary and increase quickly at Horsethief Draw and the Seff Locality ($R^2 = 0.598$; Figs. 5 and 6). $\delta^{18}\text{O}$ values rise from -8‰ to -6‰ and $\delta^{13}\text{C}$ values rise from -5‰ to -2‰ at both sites, which span from ~ 12.6 to 10.6 ka B.P.

4.2.2. Ostracodes

$\delta^{18}\text{O}$ values of ostracodes from the Coro marl carbonate in San Pedro Valley range from -9.5 to -4.4‰ (Fig. 7, Table 4). Note that these values are not corrected for biological or "vital" effects that

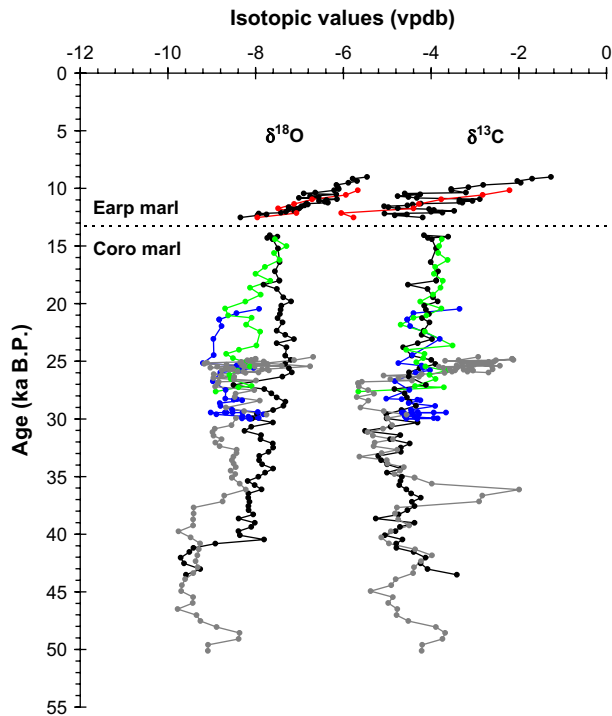


Fig. 5. Stable carbon ($\delta^{13}\text{C}$) and oxygen ($\delta^{18}\text{O}$) values of marl carbonate from Murray Springs Sections 1 (blue) and 2 (green), Horsethief Draw (black), the Seff Locality (red), and Cerros Negros (grey).

can affect stable isotope values of ostracodes (e.g., Von Grafenstein et al., 1999; Keating et al., 2002). Such vital effects are thought to vary between taxa and are not well constrained for all of the ostracodes measured in this study. Thus, to avoid problems associated with vital effects, we only compare isotopic data within a single taxon and assume that vital effects within each taxon remain constant through time.

$\delta^{18}\text{O}$ values of the ostracode calcite vary by 3–5‰ for most ostracode taxa within a single stratigraphic level. But within each taxon, there is a discernable pattern in the minimum $\delta^{18}\text{O}$ values; that is, $\delta^{18}\text{O}$ values from the early glacial period (29.5 ka B.P.) are relatively high, typically –7 to –9‰, decrease by ~1‰ across full

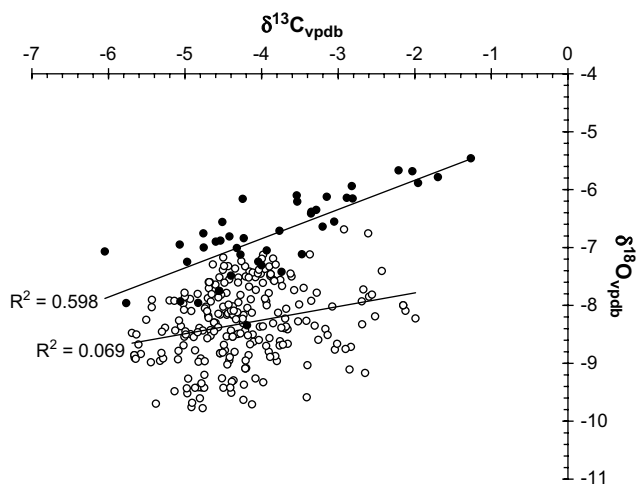


Fig. 6. $\delta^{18}\text{O}$ and $\delta^{13}\text{C}$ values for 281 measurements of carbonate from the Coro marl (open circles) and Earp marl (solid circles). Covariance of the two isotopes in the Earp marl ($R^2 = 0.598$) may reflect the presence of more stagnant water conditions, and hence more evaporation and biological productivity, between 12.6 and 10.6 ka B.P., compared to the more open-flow wetland systems represented by the older Coro marl.

glacial (24.8 ka B.P.) and LGM (20.9 ka B.P.) times, and then increase by 1–3‰ in the late glacial (15.0 ka B.P.). The $\delta^{18}\text{O}$ values of some taxa, including *Candona* sp. (large), *C. okeechobei*, and *C. vidua*, are lowest during the LGM, whereas minimum $\delta^{18}\text{O}$ values of other taxa, including *Candona* sp. (small) and *Scottia* sp., are lowest during both the full glacial and LGM. We did not find enough *S. meadensis* in stratigraphic levels below the Late Glacial to evaluate these trends.

Within a single taxon, $\delta^{13}\text{C}$ values of the ostracode calcite within a stratigraphic level vary even more, by as much as 6–7‰ (Fig. 7). Unlike the $\delta^{18}\text{O}$ values, however, we did not find any consistent trends in the minimum, maximum, or average $\delta^{13}\text{C}$ values. For example, minimum $\delta^{13}\text{C}$ values for *Candona* sp. (large) and *Scottia* sp. do not vary significantly across the full glacial or LGM, whereas minimum values for *C. stagnalis* decrease across the full glacial and $\delta^{13}\text{C}$ values for *C. okeechobei* and *C. vidua* increase across the full glacial and LGM.

We also did not find a clear relation between the $\delta^{18}\text{O}$ and $\delta^{13}\text{C}$ values of individual ostracodes. Of the seven taxa that we investigated, only *C. stagnalis* ($R^2 = 0.323$) and *S. meadensis* ($R^2 = 0.147$) showed a statistically significant relation between the two isotopes. Moreover, the slope of the $\delta^{18}\text{O}$ – $\delta^{13}\text{C}$ relation varied; some are positive (*Candona* sp. large and small, *C. stagnalis*, *C. okeechobei*, and *Scottia* sp.) and others are negative (*C. vidua* and *S. meadensis*).

5. Discussion

5.1. Depositional environment

The Coro marl was originally thought to have a lacustrine origin (Haynes, 1968), but that hypothesis has since been abandoned (Haynes, 2007c) for several reasons. First, the elevations of the marl outcrops are not uniform throughout the valley; they range from 1289 to 951 m from south to north (Table 1), which closely tracks the elevation of the San Pedro River along the same stretch of the valley. Historic tectonic activity has been observed (e.g., the 1887 Great Sonoran earthquake; Suter and Contreras (2002)), but there is no geologic evidence for tectonic activity that could have caused the hundreds of meters of tilt required to account for the modern gradient of the marl, assuming it was once uniform in elevation. Second, the uppermost elevation of the marl, 1289 m at Lehner Ranch, is positioned above two potential spillway points, into the Tucson Basin to the west via a sill between the Whetstone and Rincon Mountains and into the Gila River basin to the north via the northern San Pedro Valley (Fig. 2). The presence of a large lake in the valley would require geologic barriers at both locations. While this is certainly possible, evidence of catastrophic flooding or overflow deposits has not been observed to the west or north of the potential dam sites, nor is there any physical evidence of the dams at either location. Finally, there is no clear evidence of shorelines or depositional features in the valley as one would expect to find associated with a large lake.

An alternative hypothesis is that the Coro marl consists of a series of discontinuous ground-water discharge (GWD) deposits that were formed during a period of high water table conditions. This hypothesis is supported by several lines of evidence. First, the Coro marl deposits that have been identified are all located on the west side of the modern San Pedro River, adjacent to the high mountain ranges that flank the west side of the valley. Asymmetric distribution of GWD deposits along valley axes with deposits favoring the side with the higher mountain ranges (and thus the side with higher precipitation and increased aquifer recharge) is common elsewhere in the American Southwest (Quade et al., 1995).

Second, the mixed assemblage of high-discharge spring ostracodes (*S. meadensis*), low-flow to stagnant water ostracodes (*Heterocypris incongruens*), and spring/seep to semi-terrestrial

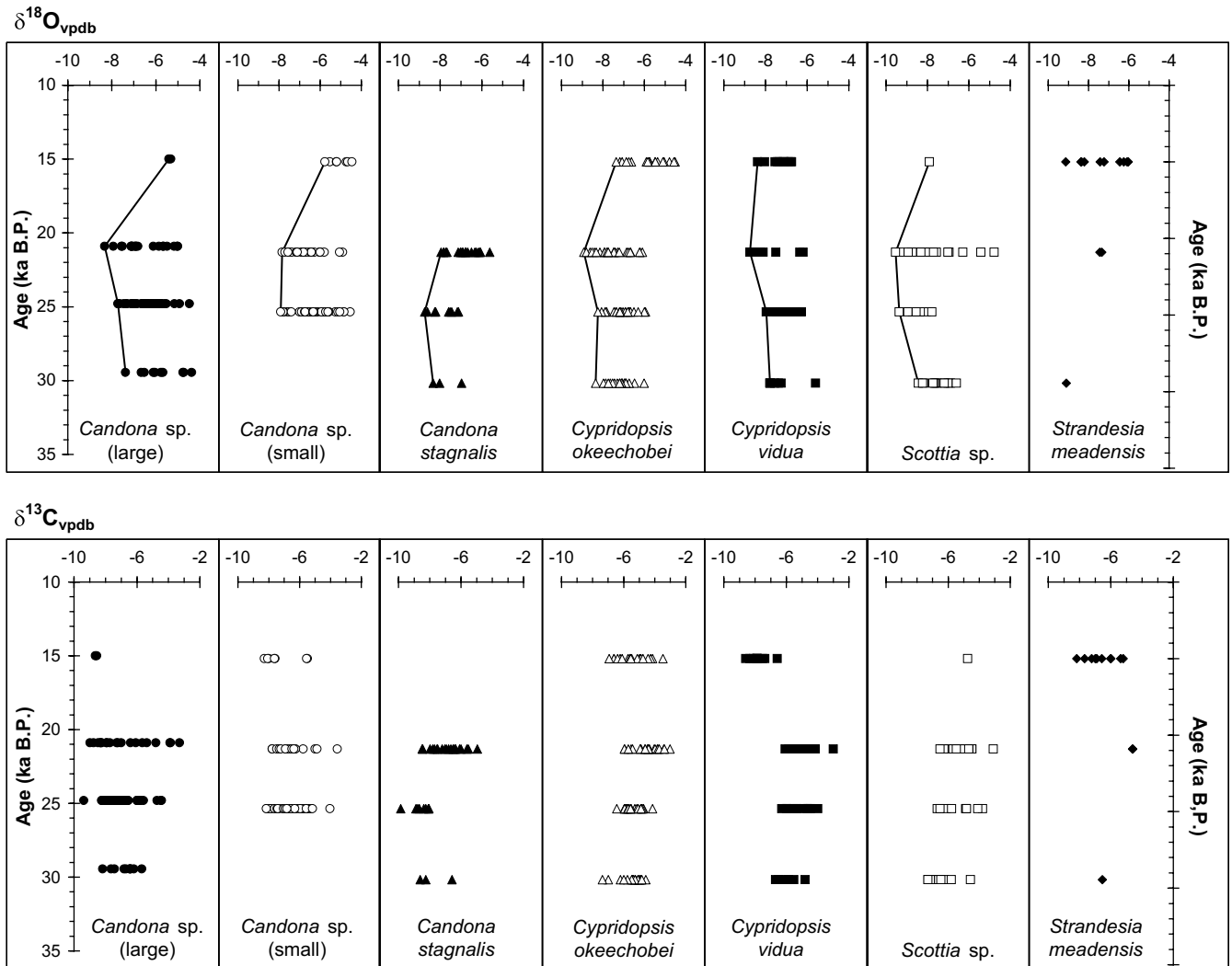


Fig. 7. $\delta^{18}\text{O}$ and $\delta^{13}\text{C}$ values for 376 measurements of ostracode calcite that represent four time periods at Murray Springs: early glacial (29.5 ka), full glacial (24.8 ka), LGM (20.9 ka), and late glacial (15.0 ka). The most negative values (connected by lines in the figure) best approximate the original isotopic composition of the host waters; more positive values are likely the result of evaporation. The distance between the spring orifices and sampled outcrops remained constant and, therefore, isotopic values within each taxon are directly comparable assuming vital effects within a given taxon do not vary with time.

ostracodes (*Scottia* sp.) are indicative, collectively, of spring complex systems, including flowing springs, wet meadows, and marshes, rather than lake systems (Forester, 1991; Külköylüoğlu and Vinyard, 2000; Külköylüoğlu, 2003; Quade et al., 2003). Similarly, the assemblages of terrestrial, semi-aquatic, and aquatic gastropods documented by Mead (1979, 2007) are indicative of a complex mosaic of wetlands, wet meadows, and spring-fed channels.

Finally, the isotopic data from both the Coro marl carbonate and the ostracodes recovered from the marl are indicative of open-system hydrologic behavior. In closed systems, such as lakes or ponds, changes in air temperatures that are accompanied by enhanced evaporation and higher biological productivity typically result in more positive $\delta^{18}\text{O}$ and $\delta^{13}\text{C}$ values that covary (Talbot, 1990). The $\delta^{18}\text{O}$ and $\delta^{13}\text{C}$ values of the Coro marl show little to no covariance ($R^2 = 0.069$; Fig. 6), nor do the stable isotopic values of the ostracode calcite (average $R^2 = 0.079$; Fig. 7, Table 4). While this evidence is indirect, it supports the idea that the Coro marl was deposited in open-system, overland-flow ciénegas or wetland settings. There may have been local ponding as found in many wetland environments today, but the isotopic values and microfaunal assemblages suggest that through-flowing conditions prevailed over much of the valley.

The Clanton clay and Earp marl were also formed during high water table conditions that prevailed in the San Pedro Valley between ~ 12.6 and 10.6 ka ago. The stable isotope results ($\delta^{18}\text{O}$, $\delta^{13}\text{C}$) of the Earp marl carbonate, however, suggest that there were significant differences between the depositional environments of the two marls. Specifically, the covariance between $\delta^{18}\text{O}$ and $\delta^{13}\text{C}$ values of the Earp marl carbonate ($R^2 = 0.598$; Fig. 6) indicates that closed-system behavior prevailed at this time. At Murray Springs and other localities, the Earp marl is associated with low-lying areas; the coeval Clanton clay is associated with adjacent higher areas. Thus, we suggest that although these younger wetland systems were also fed by high water table conditions, the Earp marl carbonate was formed in a series of shallow, evaporative ponds or pools, rather than the open-flowing ciénega systems represented by the older Coro marl.

5.2. Interpretation of stable isotopic data

The stable isotopic composition ($\delta^{13}\text{C}$, $\delta^{18}\text{O}$) of ground-water discharging from an aquifer depends on the isotopic composition of the recharge water and any isotopic changes induced during travel along the ground-water flow path. Similarly, the isotopic

Table 4
Summary of ostracode isotopic data from Murray Springs.

Section	Depth (cm)	Age (ka BP)	Parameter	<i>Candona</i> sp. (large)	<i>Candona</i> sp. (small)	<i>Candona stagnalis</i>	<i>Cypridopsis okeechobei</i>	<i>Cypridopsis vidua</i>	<i>Scottia</i> sp.	<i>Strandesia meadensis</i>
MS2	0–5	15.0	<i>n</i>	2	7	0	20	10	1	10
			$\delta^{18}\text{O}$ – max	–5.3	–4.4	–	–4.5	–6.7	–7.9	–6.0
			$\delta^{18}\text{O}$ – min	–5.4	–5.8	–	–7.4	–8.4	–7.9	–9.1
			$\delta^{13}\text{C}$ – max	–8.5	–5.5	–	–3.5	–6.6	–4.7	–5.2
			$\delta^{13}\text{C}$ – min	–8.6	–8.3	–	–6.9	–8.6	–4.7	–8.2
MS2	30–35	20.9	<i>n</i>	20	23	21	24	20	21	2
			$\delta^{18}\text{O}$ – max	–5.0	–4.9	–5.6	–6.1	–6.2	–4.8	–7.3
			$\delta^{18}\text{O}$ – min	–8.3	–7.8	–8.0	–8.9	–8.7	–9.5	–7.4
			$\delta^{13}\text{C}$ – max	–3.3	–3.5	–4.9	–2.0	–3.0	–3.1	–4.6
			$\delta^{13}\text{C}$ – min	–9.0	–10.0	–8.5	–6.0	–6.1	–6.5	–4.6
MS1	25–30	24.8	<i>n</i>	41	46	9	24	13	9	0
			$\delta^{18}\text{O}$ – max	–4.5	–4.5	–7.1	–5.9	–6.3	–7.8	–
			$\delta^{18}\text{O}$ – min	–7.7	–7.9	–8.7	–8.2	–8.0	–9.4	–
			$\delta^{13}\text{C}$ – max	–4.4	–4.0	–8.1	–4.1	–4.0	–3.8	–
			$\delta^{13}\text{C}$ – min	–9.4	–8.2	–9.9	–6.4	–6.3	–6.7	–
MS1	90–95	29.5	<i>n</i>	10	0	3	20	7	12	1
			$\delta^{18}\text{O}$ – max	–4.4	–	–7.0	–6.0	–5.6	–6.6	–9.1
			$\delta^{18}\text{O}$ – min	–7.4	–	–8.3	–8.3	–7.8	–8.4	–9.1
			$\delta^{13}\text{C}$ – max	–5.7	–	–6.6	–4.6	–4.8	–4.6	–6.5
			$\delta^{13}\text{C}$ – min	–8.2	–	–8.6	–7.4	–6.7	–7.3	–6.5
			Total <i>n</i>	73	76	33	88	50	43	13
$\delta^{13}\text{C} - \delta^{18}\text{O}$ covariance (R^2)	0.012	0.035	0.323	0.006	0.011	0.020	0.147			

composition of carbonate derived from discharge waters is a function of the isotopic composition of the water, as well as a number of other parameters (water temperature, pH, salinity, etc.). In concept, therefore, we should be able to infer changes in the isotopic composition of recharge waters by measuring the isotopic values of carbonates that ultimately derive their carbon and oxygen from those waters. This, of course, requires several assumptions: (1) minimal water–rock interaction along the ground-water flow path, (2) an absence of geothermal heating, (3) equilibrium conditions during carbonate precipitation, and (4) limited evaporation. If these conditions are satisfied, then the isotopic composition of valve carbonate of ostracodes that lived in the discharge waters, as well as carbonate precipitating from those waters (i.e., marl carbonate), could be used to determine how and when the isotopic composition of recharge waters changed over time.

A chief concern in such studies, particularly those undertaken in arid environments, is the effect of evaporation on the $\delta^{18}\text{O}$ values of the host waters. Evaporation concentrates the heavier isotope (^{18}O) in the liquid phase; the enriched $^{18}\text{O}/^{16}\text{O}$ ratios are then passed on to carbonates derived from those waters (Faure, 1991). While most wetland systems are less likely to become evaporatively enriched than lakes because they are through-flowing systems, a detailed understanding of the specific flow regime that existed at any given period of time within a wetland is often difficult to ascertain. In large valley–floor systems, such as those found in the southern Great Basin, there are multiple lines of evidence (basin morphology, sedimentary profiles, cut and fill sequences) that can be used to determine if flow-through conditions prevailed in the Pleistocene environments (Quade et al., 2003). In the San Pedro Valley, however, we cannot use the same arguments because the sediments are not as well exposed and are more limited in aerial extent. To minimize the potential impact of evaporation, therefore, we collected samples of marl carbonate that were as close to the spring vents as possible with the idea that limiting the physical distance between the paleospring vents and outcrops would limit the possibility of significant evaporation. At Murray Springs, for example, the locations of the paleospring vents have been identified and are within a few tens of meters of the marl outcrops that we sampled (Haynes, 2007c, Plate 8). The

distance between the paleosprings and marl outcrops at other sites is not as well constrained, but is assumed to be on the same scale based on the lateral distribution of marl carbonate.

Variations in the $\delta^{18}\text{O}$ and $\delta^{13}\text{C}$ values of the Coro marl carbonate are subtle, on the order of 1–2‰ over several millennia. $\delta^{18}\text{O}$ values of the marl carbonate, for example, indicate that conditions were relatively equable for most of oxygen isotope stages (OIS) 2 and 3 (Fig. 5). There is no evidence of submillennial-scale variability, such as Dansgaard–Oeschger or Heinrich events, during this period, and $\delta^{18}\text{O}$ and $\delta^{13}\text{C}$ values generally increase gradually over time with two exceptions: (1) a positive spike in $\delta^{13}\text{C}$ values at Cerros Negros that is centered at ~37 ka B.P. and, (2) positive spikes in the $\delta^{18}\text{O}$ and $\delta^{13}\text{C}$ records that are centered at ~26 ka B.P. near the top of the Cerros Negros carbonate record. The climatic or hydrologic importance of the 37 ka-spike in the Cerros Negros $\delta^{13}\text{C}$ record is unclear because it is not replicated in any of the other marl carbonate $\delta^{13}\text{C}$ records. It may reflect a brief change in the isotopic composition of the dissolved inorganic carbon (DIC) of the discharge waters at Cerros Negros, a temporary change in the biological productivity at this location, or another local effect that did not impact hydrologic systems farther south in the San Pedro Valley. The spike in oxygen and carbon isotopic values near the top of the Cerros Negros carbonate record likely reflects diagenetic processes, such as pedogenic overprinting, as the top of the Coro marl is exposed at the surface at this location.

Minimum $\delta^{18}\text{O}$ values in the ostracodes recovered from Murray Springs exhibit a modest (~1‰) decrease across full glacial and LGM times. The more negative $\delta^{18}\text{O}$ values are likely the result of the “rain-out effect” in which heavier nuclides are preferentially removed during successive precipitation events via Rayleigh distillation; the magnitude of the rain out effect is enhanced as temperatures decrease because fractionation of oxygen isotopes is greater at lower temperatures. The net result is that ostracode calcite records lower or more negative $\delta^{18}\text{O}$ values during periods of cooler and/or moister conditions. As discussed above, it is not possible to relate the modest decrease in the $\delta^{18}\text{O}$ values of the ostracode calcite across full glacial and LGM times quantitatively to climate parameters (P/ET) because of the open-system nature of wetland systems.

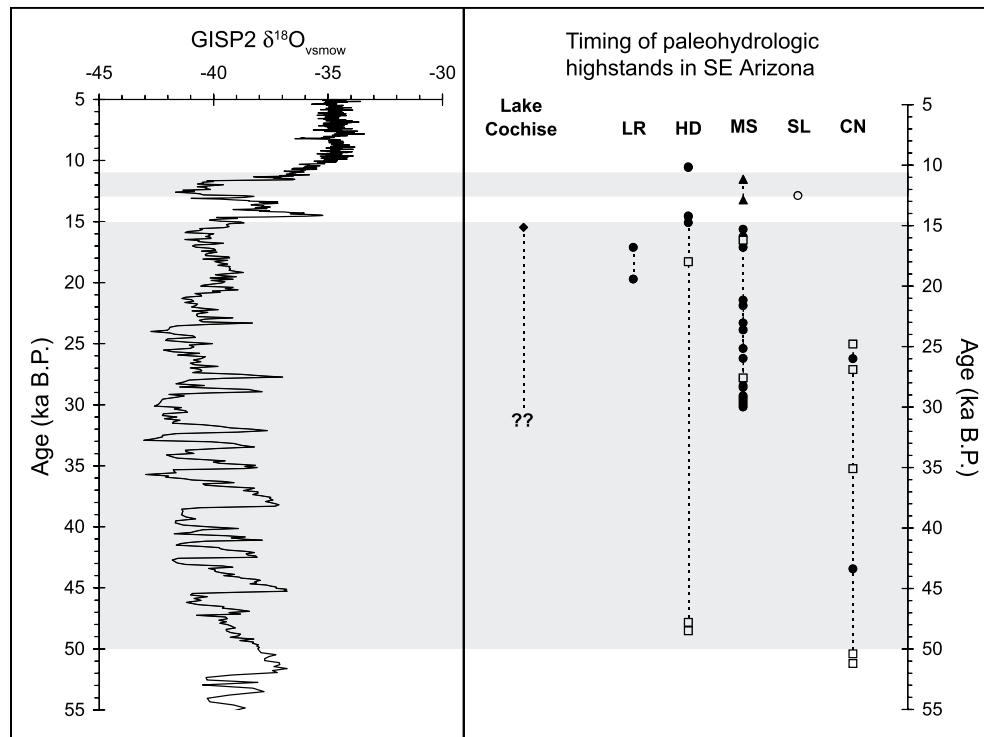


Fig. 8. Comparison of the timing of variations in the GISP2 $\delta^{18}O$ record and paleohydrologic records from southeast Arizona, including pluvial Lake Cochise (Waters, 1989) and the San Pedro Valley GWD deposits. In the right panel, solid diamonds denote ages based on ^{14}C dating of charcoal, solid circles denote ages based on ^{14}C dating of small terrestrial gastropods, solid triangles denote ages based on ^{14}C dating of organic matter, and open squares denote luminescence ages. Shaded intervals represent high-water table conditions in the San Pedro Valley for comparison with the GISP2 $\delta^{18}O$ record. Upper and lower limits of these conditions are defined by the midpoint of the limiting ages at Horsethief Draw, Murray Springs, and the Seff Locality (see text for discussion). Warming in the North Atlantic at the onset of the Bølling–Allerød warm period broadly coincides with abandonment of the 1274-m shoreline at pluvial Lake Cochise and a drop in the regional water table in the San Pedro Valley. A return to cooler conditions during the Younger Dryas cold event in the North Atlantic was accompanied by a temporary rise in the regional water table and deposition of the Clanton clay and Earp marl in the valley.

5.3. Paleohydrology of southeastern Arizona

One of the major assumptions in paleohydrologic research is that changes in climate affect all aspects of the hydrologic cycle of an area simultaneously. In other words, different sources of paleohydrologic information from a region should yield similar results. In southeastern Arizona, we have the unusual opportunity to test this assumption by comparing the timing of changes in the local or regional hydrologic budget as reconstructed by the San Pedro Valley GWD deposits, a speleothem calcite $\delta^{18}O$ record from nearby Cave of the Bells (COB) that is located in the Santa Rita Mountains ~40 km west of the San Pedro Valley (Wagner, 2006), and a lake highstand record from Pluvial Lake Cochise, located ~30 km east of the San Pedro Valley where Willcox Playa exists today (Waters, 1989) (Fig. 2).

Deposition of the Coro marl indicates that ground-water levels in the San Pedro Valley were high between ~50 and 14.7 ka B.P., fell and remained low as erosive conditions dominated the region until 12.6 ka B.P., rebounded briefly between ~12.6 and 10.6 ka B.P. as evidenced by deposition of the Clanton clay and Earp marl, and then fell again and remained low throughout the Holocene. $\delta^{18}O$ values of ostracode calcite at Murray Springs also suggest that climate conditions between ~25 and 20 ka B.P. were cooler and/or moister than conditions either before or after this period. Similarly, the COB speleothem $\delta^{18}O$ record shows large changes at ~50 ka B.P. (negative), ~15 ka B.P. (positive), ~13 ka B.P. (negative), and ~11 ka B.P. (positive), similar to the timing of changes in water table levels recorded by the GWD deposits. Moreover, the isotopic changes in the COB speleothem record between ~25 and 20 ka B.P. are roughly coincident, in the same direction, and are approximately the same magnitude as changes in the $\delta^{18}O$ record of the

ostracode calcite from the San Pedro Valley. Finally, the timing of the drop in ground-water levels in the San Pedro Valley at ~15 ka B.P. coincides with abandonment of the 1274-m lake highstand at pluvial Lake Cochise (Waters, 1989).

In southeastern Arizona, therefore, the assumption that different hydrologic records should yield similar results regarding the nature and timing of climate change appears to be validated as ground-water and pluvial lake levels in this region were directly linked with changes in climate (Fig. 8). At ~50 ka B.P., ground-water levels in the San Pedro Valley rose as climate conditions became cool and/or moist, initiating deposition of the Coro marl in discontinuous ciénegas through the valley. Ground-water levels remained high for the next ~35 ka until climate abruptly shifted toward warm and/or dry conditions as indicated by positive excursion of $\delta^{18}O$ values in the COB speleothem. This transition is also recorded by the abandonment of the 1274-m highstand at pluvial Lake Cochise. Ground-water levels remained low between ~14.7 and 12.6 ka B.P. and erosive conditions prevailed in the valley as climate remained warm and/or dry during the Bølling–Allerød warm period and Clovis-age drought of Haynes (1991). Approximately coincident with the onset of the Younger Dryas cold event, ground-water levels in the San Pedro Valley rebounded, which fed the springs and shallow ponds in which the Clanton clay and Earp marl were deposited. At the onset of the Holocene, ~10.6 ka B.P., ground-water levels in the valley fell once again as climate abruptly shifted back to warm and/or dry conditions as seen in the COB speleothem record. Unlike the previous hydrologic changes, this transition was also accompanied by a major shift in vegetation regimes in the Sonoran and Chihuahuan Deserts (e.g., Van Devender et al., 1987, and references therein). There is no evidence of a return to high water table conditions in the San Pedro

Valley, which suggests that warm temperatures, low precipitation rates, and erosive conditions prevailed in southeastern Arizona since the onset of the Holocene.

The timing of the hydrologic changes in the San Pedro Valley coincide broadly with variations in the GISP2 $\delta^{18}\text{O}$ record (Fig. 8), which supports the hypothesis that atmospheric teleconnections existed between the North Atlantic and the American Southwest during the late Pleistocene. However, we note that we did not observe any evidence of submillennial-scale variability, such as Dansgaard–Oeschger or Heinrich events, in the sediments or isotopic data of the GWD deposits in the San Pedro Valley. Such short-term fluctuations in climate conditions either did not occur in southern Arizona or, more likely, the effect of such fluctuations was lost to bioturbation or other processes related to marl deposition. Evidence of atmospheric teleconnections linking the North Atlantic and the American Southwest has been documented previously in high-resolution records from coastal marine settings (Kennett and Ingram, 1995; Hendy et al., 2002), speleothems (Polyak et al., 2004), and lake records (e.g., Phillips et al., 1994; Benson et al., 1997), but to our knowledge this is the first record of GWD deposits that supports the existence of climate teleconnections between these regions during the Pleistocene.

On a finer, more detailed scale, it is unclear how far geographically we can confidently project the paleohydrologic record that we have developed in southeastern Arizona. For example, did ground-water tables in the eastern Chihuahuan Desert or in northern Mexico rise and fall in unison with those in San Pedro Valley? When and how did hydrologic systems in the northern Great Basin and Colorado Plateau respond to climate change? And is there evidence in these areas of ground-water highstands related to regional aquifers during the Holocene? Future work, including the development of systematic transects of paleohydrologic information across the American Southwest, may allow us to address these issues. Much like the spatial arrays of packrat midden and pollen records that have been developed over the last few decades, we foresee the use of paleohydrologic records to establish the timing and magnitude of past hydrologic change on local to regional scales across the Southwest. GWD deposits have the potential to play a major role in this effort and may provide detailed insight into how hydrologic systems, specifically small desert watersheds, responded to past climate change on a variety of spatial and temporal scales.

6. Conclusions

Ground-water discharge (GWD) deposits reflect past episodes of high-water table conditions that prevailed throughout the deserts of the American Southwest during the late Pleistocene. GWD deposits directly record the minimum height of past highstands of local or regional ground-water tables, and can be accurately dated using a variety of chronometric techniques, including radiocarbon dating of terrestrial gastropod shells and luminescence dating.

GWD deposits in the San Pedro Valley of southeastern Arizona include two carbonate-rich units, the Coro and Earp marls, and the Clanton clay (black mat), which are found in discontinuous sediment packages over a ~150-km stretch of the valley between the U.S.–Mexico border and the Gila River Basin to the north. Sedimentological, isotopic, and microfaunal assemblages collectively suggest that these deposits were formed in a series of discontinuous ciénegas and wetland systems during the late Pleistocene. Water tables in the valley began to rise in response to climate change ~50 ka B.P., and remained high for ~35 ka until an abrupt shift in climate toward warm and/or dry conditions occurred during the Bølling–Allerød warm period, ~15 ka B.P. Water table elevations then rebounded briefly during the Younger Dryas cold event before falling at the onset of the Holocene. There is no

evidence of additional ground-water highstands during the remainder of the Holocene.

The timing of the changes in water table elevations in the San Pedro Valley during the late Pleistocene coincide with abrupt changes in oxygen isotopic values in speleothem calcite from Cave of Bells to the west of the valley and the abandonment of a lake highstand at pluvial Lake Cochise to the east. Thus, in southeastern Arizona, the assumption that changes in climate are reflected in all aspects of the hydrologic cycle of a region simultaneously is validated. In addition, the timing of these hydrologic changes is broadly coincident with variations in the GISP2 ice core record, which supports the hypothesis that atmospheric teleconnections existed between the North Atlantic and the deserts of the American Southwest during the late Pleistocene.

Acknowledgments

We thank W. Pratt and J. Nekola for their assistance with gastropod identifications. We also thank E. Pigati for field assistance and D. Dettman and J. Budahn for laboratory assistance. We also thank the Arizona AMS facility, particularly A.J.T. Jull, for providing many of the radiocarbon measurements at reduced cost. This project benefited tremendously from insightful conversations with C.V. Haynes, Jr., J. Quade, and J. Betancourt, and the support of L. Klasky and the University of Arizona Desert Laboratory. This manuscript also improved through constructive reviews from G. Ellis, M. Kirby, D. Muhs, R. Thompson, and an anonymous reviewer. This project was funded in part by the U.S. Geological Survey's Mendenhall post-doctoral research program.

Appendix A. Supplementary data

Supplementary data associated with this article can be found in the online version, at doi:10.1016/j.quascirev.2008.09.022.

References

- Aitken, M.J., 1985. Thermoluminescence Dating. Academic Press, London, 359 pp.
- Allen, B.D., Anderson, R.Y., 2000. A continuous, high-resolution record of late Pleistocene climate variability from the Estancia basin, New Mexico. Geological Society of America Bulletin 112, 1444–1458.
- Anderson, R.S., Van Devender, T.R., 1991. Comparison of pollen and macrofossils in packrat (*Neotoma*) middens; a chronological sequence from the Waterman Mountains of southern Arizona, U.S.A. Review of Palaeobotany and Palynology 68, 1–28.
- Ashbaugh, K.M., Metcalf, A.L., 1986. Fossil molluscan faunas from four spring-related deposits in the northern Chihuahuan Desert, southern New Mexico, and westernmost Texas. New Mexico Bureau of Mines and Mineral Resources 200, 5–25.
- Bartlein, P.J., Anderson, K.H., Anderson, P.M., Edwards, M.E., Mock, C.J., Thompson, R.S., Webb, R.S., Whitlock, C., 1998. Paleoclimate simulations for North America over the past 21,000 years: features of the simulated climate and comparisons with paleoenvironmental data. Quaternary Science Reviews 17, 549–585.
- Benson, L., Burdett, J., Lund, S., Kashgarian, M., Mensin, S., 1997. Nearly synchronous climate change in the northern hemisphere during the last glacial termination. Nature 388, 263–265.
- Betancourt, J.L., Rylander, K.A., Peñalba, C., McVickar, J.L., 2001. Late Quaternary vegetation history of Rough Canyon, south-central New Mexico, USA. Palaeogeography, Palaeoclimatology, Palaeoecology 165, 71–95.
- COHMAP, 1988. Climatic changes of the last 18,000 years – observations and model simulations. Science 241, 1043–1052.
- Cooke, R.U., Reeves, R.W., 1976. Arroyos and Environmental Change. Oxford University Press, Oxford, 213 pp.
- Deevey, E.S.J., Gross, M.S., Hutchinson, G.E., Kraybill, H.L., 1954. The natural ^{14}C contents of materials from hard-water lakes. Proceedings of the National Academy of Science 40, 285–288.
- Fairbanks, R.G., Mortlock, R.A., Chiu, T.-C., Cao, L., Kaplan, A., Guilderson, T.P., Fairbanks, T.W., Bloom, A.L., 2005. Marine radiocarbon calibration curve spanning 0 to 50,000 years B.P. based on paired $^{230}\text{Th}/^{234}\text{U}/^{238}\text{U}$ and ^{14}C dates on pristine corals. Quaternary Science Reviews 24, 1781–1796.
- Faure, G., 1991. Principles and Applications of Inorganic Geochemistry. Macmillan Publishing Company, New York, NY, 626 pp.
- Fleischhauer, H.L.J., Stone, W.J., 1982. Quaternary geology of Lake Animas, Hidalgo County, New Mexico. New Mexico Bureau of Mines and Mineral Resources Circular 174, 1–25.

- Forester, R.M., 1991. Ostracode assemblages from springs in the western United States: implications for paleohydrology. *Memoirs of the Entomological Society of Canada* 155, 181–201.
- Forester, R.M., Miller, D.M., Pedone, V., 2003. Ground water and ground-water discharge carbonate: deposits in warm deserts. In: Reynolds, R.E. (Ed.), *Land of Lost Lakes: the 2003 Desert Symposium Field Trip*. California State University, Desert Studies Consortium, pp. 27–36.
- Forman, S.L., Pierson, J., 2002. Late Pleistocene luminescence chronology of loess deposition in the Missouri and Mississippi river valleys, United States. *Palaeogeography, Palaeoclimatology, Palaeoecology* 186, 25–46.
- Geyh, M.A., Schotterer, U., Grosjean, M., 1998. Temporal changes of the ^{14}C reservoir effect in lakes. *Radiocarbon* 40, 921–931.
- Goodfriend, G.A., Stipp, J.J., 1983. Limestone and the problem of radiocarbon dating of land-snail shell carbonate. *Geology* 11, 575–577.
- Hanson, R.B., 2001. *The San Pedro River: a Discovery Guide*. The University of Arizona Press, Tucson, 205 pp.
- Harris, A.H., 1987. Reconstruction of mid-Wisconsin environments in southern New Mexico. *National Geographic Research* 3, 142–151.
- Haury, E.W., Antevs, E., Lance, J.F., 1953. Artifacts with mammoth remains, Naco, Arizona. *American Antiquity* 19, 1–24.
- Haury, E.W., Sayles, E.B., Wasley, W.W., 1959. The Lehner mammoth site, south-eastern Arizona. *American Antiquity* 25, 2–30.
- Haynes Jr., C.V., 1968. Preliminary report on the late Quaternary geology of the San Pedro Valley, Arizona. In: Tittle, S.R. (Ed.), *Southern Arizona Guidebook III*. Arizona Geological Society, Tucson, pp. 79–96.
- Haynes Jr., C.V., 1984. Stratigraphy and late Pleistocene extinction in the United States. In: Martin, P.S., Klein, R.G. (Eds.), *Quaternary Extinctions: a Prehistoric Revolution*. The University of Arizona Press, Tucson, pp. 345–353.
- Haynes Jr., C.V., 1987. Curry Draw, Cochise County, Arizona: a late Quaternary stratigraphic record of Pleistocene extinction and paleo-Indian activities. *Geological Society of America Centennial Field Guide – Cordilleran Section* 6, 23–28.
- Haynes Jr., C.V., 1991. Geoaerchaeological and paleohydrological evidence for a Clovis-age drought in North America and its bearing on extinction. *Quaternary Research* 35, 438–450.
- Haynes, C.V., Jr., 1998. Stratigraphic manifestations of paleoclimatic events at Paleoindian sites: geochronology of the Pleistocene–Holocene transition and megafauna extinction. In: 63rd Annual Meeting of the Society for American Archaeology (SAA), Seattle, WA, 138.
- Haynes Jr., C.V., 2007a. Appendix A: radiocarbon dating at Murray Springs and Curry Draw. In: Haynes Jr., C.V., Huckell, B.B. (Eds.), *Murray Springs: a Clovis Site with Multiple Activity Areas in the San Pedro Valley, Arizona*. The University of Arizona Press, Tucson, pp. 229–239.
- Haynes Jr., C.V., 2007b. Appendix B: nature and origin of the black mat, stratum F2. In: Haynes Jr., C.V., Huckell, B.B. (Eds.), *Murray Springs: a Clovis Site with Multiple Activity Areas in the San Pedro Valley, Arizona*. The University of Arizona Press, Tucson, pp. 240–249.
- Haynes Jr., C.V., 2007c. Quaternary geology of the Murray Springs Clovis site. In: Haynes Jr., C.V., Huckell, B.B. (Eds.), *Murray Springs: a Clovis Site with Multiple Activity Areas in the San Pedro Valley, Arizona*. The University of Arizona Press, Tucson, pp. 16–56.
- Haynes Jr., C.V., Huckell, B.B., 2007. Murray Springs: a Clovis Site with Multiple Activity Areas in the San Pedro Valley, Arizona. The University of Arizona Press, Tucson, 308 pp.
- Hemmings, E.T., 2007. Buried animal kills and processing localities, Areas 1–5. In: Haynes Jr., C.V., Huckell, B.B. (Eds.), *Murray Springs: a Clovis Site with Multiple Activity Areas in the San Pedro Valley, Arizona*. The University of Arizona Press, Tucson, pp. 83–137.
- Hemmings, E.T., Haynes Jr., C.V., 1969. The Escapule mammoth and associated projectile points, San Pedro Valley, Arizona. *Journal of the Arizona Academy of Science* 5, 184–188.
- Hendy, I.L., Kennett, J.P., Roark, E.B., Ingram, B.L., 2002. Apparent synchronicity of submillennial scale climate events between Greenland and Santa Barbara Basin, California from 30 to 10 ka. *Quaternary Science Reviews* 21, 1167–1184.
- Holmgren, C.A., Betancourt, J.L., Rylander, K.A., 2006. A 36,000-yr vegetation history from the Peloncillo Mountains, southeastern Arizona, USA. *Palaeogeography, Palaeoclimatology, Palaeoecology* 240, 405–422.
- Holmgren, C.A., Peñalba, M.C., Rylander, K.A., Betancourt, J.L., 2003. A 16,000 ^{14}C yr B.P. packrat midden series from the USA–Mexico Borderlands. *Quaternary Research* 60, 319–329.
- Huntley, D.J., Lamothe, M., 2001. Ubiquity of anomalous fading in K-feldspars and the measurement and correction for it in optical dating. *Canadian Journal of Earth Sciences* 38, 1093–1106.
- Karlen, I., Olsson, I.U., 1962. A new determination of the half-life of carbon-14 with a proportional counter. *Arkiv for Fysik* 22, 416–417.
- Kaufman, D.S., O'Brien, G., Mead, J.L., Bright, J., Umhoefer, P., 2002. Late Quaternary spring-fed deposits of the Grand Canyon and their implication for deep lava-dammed lakes. *Quaternary Research* 58, 329–340.
- Keating, K.W., Heaton, T.H.E., Holmes, J.A., 2002. Carbon and oxygen isotope fractionation in non-marine ostracodes: results from a 'natural culture' environment. *Geochimica et Cosmochimica Acta* 66, 1701–1711.
- Kennett, J.P., Ingram, B.L., 1995. A 20,000-year record of ocean circulation and climate change from the Santa Barbara Basin. *Nature* 377, 510–514.
- King, J.E., Van Devender, T.R., 1977. Pollen analysis of fossil packrat middens from the Sonoran Desert. *Quaternary Research* 8, 191–204.
- Krider, P.R., 1998. Paleoclimatic significance of late Quaternary lacustrine and alluvial stratigraphy, Animas Valley, New Mexico. *Quaternary Research* 50, 283–289.
- Külkölüglü, O., 2003. A new report on the loss of *Scottia pseudobrowniana* Kempf, 1971 (Ostracoda) from a limnocene spring in Bolu, Turkey. *Crustaceana* 76, 257–268.
- Külkölüglü, O., Vinyard, G.L., 2000. Distribution and ecology of freshwater ostracoda (*Crustacea*) collected from springs of Nevada, Idaho, and Oregon: a preliminary study. *Western North American Naturalist* 60, 291–303.
- Kutzbach, J., Gallimore, R., Harrison, S., Behling, P., Selin, R., Laarif, F., 1998. Climate and biome simulations for the past 21,000 years. *Quaternary Science Reviews* 17, 473–506.
- Lang, A., 1994. Infrared stimulated luminescence dating of Holocene reworked silty sediments. *Quaternary Science Reviews* 13, 525–528.
- Libby, W.F., 1955. *Radiocarbon Dating*. University of Chicago Press, Chicago, 175 pp.
- Long, A., 1966. Late Pleistocene and Recent Chronologies of Play Lakes in Arizona and New Mexico. Unpublished Ph.D. thesis, University of Arizona, 141 pp.
- Mahan, S.A., Miller, D.M., Menges, C.M., Yount, J.C., 2007. Late Quaternary stratigraphy and luminescence geochronology of the northeastern Mojave Desert. *Quaternary International* 166, 61–78.
- Mann, W.B., Marlow, W.F., Hughes, E.E., 1961. Half-life of carbon-14. *International Journal of Applied Radiation and Isotopes* 11, 57.
- McAuliffe, J.R., Van Devender, T.R., 1998. A 22,000-year record of vegetation change in the north-central Sonoran Desert. *Palaeogeography, Palaeoclimatology, Palaeoecology* 141, 253–275.
- Mead, J.L., 1979. The late Pleistocene and Holocene molluscs of the Murray Springs Clovis site, Arizona. Unpublished M.S. thesis, University of Arizona, 40 pp.
- Mead, J.L., 2007. Molluscan faunas of the San Pedro Valley, Arizona. In: Haynes Jr., C.V., Huckell, B.B. (Eds.), *Murray Springs: a Clovis Site with Multiple Activity Areas in the San Pedro Valley, Arizona*. The University of Arizona Press, Tucson, pp. 62–82.
- Mead, J.L., Haynes Jr., C.V., Huckell, B.B., 1975. A late Pleistocene mastodon (*Mammuth americanum*) from the Lehner site, southeastern Arizona. *The Southwestern Naturalist* 24, 231–238.
- Minckley, T.A., Brunelle, A., 2007. Paleohydrology and growth of a desert ciénega. *Journal of Arid Environments* 69, 420–431.
- Pedone, V., Rivera, K., 2003. Groundwater-discharge deposits in Fenner Wash, eastern Mojave Desert. *Geological Society of America Abstracts with Programs* 35, 257.
- Phillips, F.M., Campbell, A.R., Smith, G.I., Bischoff, J.L., 1994. Interstadial climatic cycles: a link between western North America and Greenland? *Geology* 22, 1115–1118.
- Pigati, J.S., Quade, J., Shanahan, T.M., Haynes Jr., C.V., 2004. Radiocarbon dating of minute gastropods and new constraints on the timing of spring-discharge deposits in southern Arizona, USA. *Palaeogeography, Palaeoclimatology, Palaeoecology* 204, 33–45.
- Placzek, C., Quade, J., Patchett, P.J., 2006. Geochronology and stratigraphy of late Pleistocene lake cycles on the southern Bolivian Altiplano: implications for causes of tropical climate change. *Geological Society of America Bulletin* 118, 515–532.
- Polyak, V.J., Rasmussen, J.B.T., Asmerom, Y., 2004. Prolonged wet period in the southwestern United States through the Younger Dryas. *Geology* 32, 5–8.
- Pool, D.R., Coes, A.L., 1999. Hydrogeologic investigations of the Sierra Vista watershed of the Upper San Pedro Basin, Cochise County, Southeast Arizona. U.S. Geological Survey Water-Resources Investigations Report 99-4197, 1–41.
- Prescott, J.R., Hutton, J.T., 1994. Cosmic ray contributions to dose rates for luminescence and ESR dating: large depths and long-term time variations. *Radiation Measurements* 23, 497–500.
- Quade, J., 1986. Late Quaternary environmental changes in the upper Las Vegas Valley, Nevada. *Quaternary Research* 26, 340–357.
- Quade, J., Forester, R.M., Pratt, W.L., Carter, C., 1998. Black mats, spring-fed streams, and late-glacial-age recharge in the southern Great Basin. *Quaternary Research* 49, 129–148.
- Quade, J., Forester, R.M., Whelan, J.F., 2003. Late Quaternary paleohydrologic and paleotemperature change in southern Nevada. In: *Paleoenvironments and Paleohydrology of the Mojave and Southern Great Basin Deserts*, vol. 368. Geological Society of America Bulletin Special Paper, 368 pp. 165–188.
- Quade, J., Miffiin, M.D., Pratt, W.L., McCoy, W.D., Burckle, L., 1995. Fossil spring deposits in the southern Great Basin and their implications for changes in water-table levels near Yucca Mountain, Nevada, during Quaternary time. *Geological Society of America Bulletin* 107, 213–230.
- Quade, J., Pratt, W.L., 1989. Late Wisconsin groundwater discharge environments of the Southwestern Indian Springs Valley, southern Nevada. *Quaternary Research* 31, 351–370.
- Ratkevich, R.P., 1993. Camel recovery in southern Arizona: a preliminary report. In: *First Annual Symposium Fossils of Arizona*, Mesa Southwest Museum and Southwest Paleontological Society, Tucson, AZ, pp. 80–85.
- Reimer, P.J., Baillie, M.G.L., Bard, E., Bayliss, A., Beck, J.W., Bertrand, C.J.H., Blackwell, P.G., Buck, C.E., Burr, G.S., Cutler, K.B., Damon, P.E., Edwards, R.L., Fairbanks, R.G., Friedrich, M., Guilderson, T.P., Hogg, A.G., Hughen, K.A., Kromer, B., McCormac, F.G., Manning, S.W., Ramsey, C.B., Reimer, R.W., Remmele, S., Southon, J.R., Stuiver, M., Talamo, S., Taylor, F.W., van der Plicht, J., Weyhenmeyer, C.E., 2004. IntCal04 terrestrial radiocarbon age calibration, 0–26 ka cal BP. *Radiocarbon* 46, 1029–1058.
- Restrepo, J.L., Montoya, A.M., Obeysekera, J., 1998. A wetland simulation module for the MODFLOW ground water model. *Ground Water* 36, 764–770.
- Reynolds, S.J., 1988. *Geologic Map of Arizona*. Arizona Geological Survey Map 26. Scale 1:1,000,000.

- Richardson, C.A., McDonald, E.V., Busacca, A.J., 1997. Luminescence dating of loess from the northwest United States. *Quaternary Science Reviews* 16, 403–415.
- Riggs, A.C., 1984. Major carbon-14 deficiency in modern snail shells from southern Nevada springs. *Science* 224, 58–61.
- Singhvi, A.K., Sharma, Y.P., Agrawal, D.P., 1982. Thermo-luminescence dating of sand dunes in Rajasthan, India. *Nature* 295, 313–315.
- Stuiver, M., Reimer, P.J., 1993. Extended ^{14}C database and revised CALIB radiocarbon calibration program. *Radiocarbon* 35, 215–230.
- Suter, M., Contreras, J., 2002. Active tectonics of northeastern Sonora, Mexico (southern Basin and Range Province) and the 3 May 1887 M_w 7.4 Earthquakes. *Bulletin of the Seismological Society of America* 92, 581–589.
- Talbot, M.R., 1990. A review of the paleohydrological interpretation of carbon and oxygen isotopic ratios in primary lacustrine carbonates. *Chemical Geology (Isotope Geoscience Section)* 80, 261–279.
- Thompson, R.S., Whitlock, C., Bartlein, P.J., Harrison, S.P., Spaulding, W.G., 1993. Climatic changes in the western United States since 18,000 yr B.P. In: Wright Jr., H.E., Kutzbach, J.E., Webb III, T., Ruddiman, W.F., Street-Perrott, F.A., Bartlein, P.J. (Eds.), *Global Climates Since the Last Glacial Maximum*. University of Minnesota Press, Minneapolis, pp. 468–513.
- Van Devender, T.R., 1990a. Late Quaternary vegetation and climate of the Chihuahuan Desert, United States and Mexico. In: Betancourt, J.L., Van Devender, T.R., Martin, P.S. (Eds.), *Packrat Middens; the Last 40,000 years of Biotic Change*. University of Arizona Press, Tucson, AZ, pp. 104–133.
- Van Devender, T.R., 1990b. Late Quaternary vegetation and climate of the Sonoran Desert, United States and Mexico. In: Betancourt, J.L., Van Devender, T.R., Martin, P.S. (Eds.), *Packrat Middens; the Last 40,000 years of Biotic Change*. University of Arizona Press, Tucson, AZ, pp. 134–165.
- Van Devender, T.R., Burgess, T.L., 1985. Late Pleistocene woodlands in the Bolson de Mapimi: a refugium for the Chihuahuan desert biota? *Quaternary Research* 24, 346–353.
- Van Devender, T.R., Thompson, R.S., Betancourt, J.L., 1987. Vegetation history of the deserts of southwestern North America; the nature and timing of the late Wisconsin–Holocene transition. In: Ruddiman, W.F., Wright, H.E. (Eds.), *North America and Adjacent Oceans During the Last Deglaciation*. Geological Society of America, Boulder, CO, pp. 323–352.
- Von Grafenstein, U., Erlener, H., Trumborn, P., 1999. Oxygen and carbon isotopes in modern fresh-water ostracode valves: assessing vital offsets and autoecological effects of interest for paleoclimate studies. *Palaeogeography, Palaeoclimatology, Palaeoecology* 148, 133–152.
- Wagner, J.D.M., 2006. Speleothem record of southern Arizona paleoclimate, 54 to 3.5 ka. Unpublished Ph.D. thesis, University of Arizona, 129 pp.
- Waters, M.R., 1989. Late Quaternary lacustrine history and paleoclimatic significance of pluvial Lake Cochise, southeastern Arizona. *Quaternary Research* 32, 1–11.
- Waters, M.R., Haynes, C.V., 2001. Late Quaternary arroyo formation and climate change in the American Southwest. *Geology* 29, 399–402.
- Watt, D.E., Ramsden, D., Wilson, H., 1961. Half-life of carbon-14. *International Journal of Applied Radiation and Isotopes* 11, 68.
- Wilkins, D.E., Currey, D.R., 1997. Timing and extent of late Quaternary paleolakes in the Trans-Pecos closed basin, west Texas and south-central New Mexico. *Quaternary Research* 47, 306–315.